Involvement of the alPFC in electroencephalographic processes that underlie fear processing and fear downregulation: a TMS-EEG study

Marián Boor[1], Sanne C. Rodenburg[1], Johanna M.P. Baas[1]

[1]Department of Experimental Psychology, Utrecht University, the Netherlands

Corresponding author: M. Boor, Email: m.boor1@students.uu.nl, J.M.P. Baas, Email: j.m.p.baas@uu.nl

Contents

Abstract

It is necessary to downregulate fear after threat termination to prevent chronic anxiety. The anterolateral prefrontal cortex (alPFC) has been found to play a role in fear downregulation and in the regulation of emotional behavior. EEG research has shown that fronto-medial theta is involved in fear expression. Theta oscillations are also involved in cognitive reappraisal and alPFC-theta has been found to be associated with the control of emotional actions. By applying cTBS over the alPFC, we can causally study the involvement of the alPFC in fear downregulation and its influence on oscillatory mechanisms that underlie this process. Healthy participants (N=30) completed an instructed fear task before and after receiving active (alPFC) and control (vertex) cTBS. We found no effect of cTBS on theta oscillations. Against our hypothesis, we did not find a difference between the threat and safe cue in theta oscillations after cue onset. However, a difference between cue conditions was found in the delta range. After cue offset, higher theta power was found in the threat versus safe condition. In conclusion, theta oscillations were not involved in fear expression during the presentation of the cue, but they were associated with either fear expression or fear downregulation after cue offset. Our study provides additional evidence for the involvement of delta oscillations in emotional processing. It remains unclear whether the lack of cTBS effect is caused by an insufficient involvement of alPFC in fear processing, if the brain changes induced by the cTBS over alPFC were not captured by theta oscillations, or if the cTBS did not influence the brain.

Layman's Summary

After a threat has disappeared, it is necessary to downregulate fear to prevent chronic anxiety. A frontal brain area called the anterolateral prefrontal cortex (alPFC) has been found to be involved in regulating emotional behavior and downregulating fear. Studies that record electrical brain activity have found that brainwaves in the theta range (4 to 8 Hz) measured in the frontal middle brain areas are associated with fear processing. Theta brainwaves measured in these locations have been found to originate in a brain region called the dorsomedial PFC (dmPFC), which is involved in fear expression. However, theta brainwaves originating in the alPFC have been found to be involved in the process of regulating social emotional behavior. In our study, we used brain stimulation that decreases the activity in the targeted brain area. By targeting the alPFC, we can directly study the causal involvement of this brain area in downregulating fear and the underlying electrical activity involved in this process. We recruited 30 healthy participants that completed a task, in which they were instructed that they may receive an electric shock when they are presented with one cue (threat cue), whereas they would never receive an electric shock when presented with another cue (safe cue). Against our expectations, we did not find any effect of the brain stimulation on theta brainwaves. During the presentation of the cue, there was no difference between the threatening and the safe cue in the theta brainwaves. However, we did find a difference between these conditions in slower brainwave band called delta (0.5 to 4 Hz). The threatening condition induced stronger delta brainwaves than the safe condition. Delta brainwaves have been found to play a role in emotional processing and therefore, the stronger delta during threatening versus the safe cue can be explained by stronger emotional processing elicited by the threatening stimulus. After the cue disappeared, we did find a difference between the threatening and the safe cue in theta brainwaves, with the threatening condition having stronger theta waves than the safe condition. However, it is unclear whether this theta increase represents the process of fear downregulation,

or the ongoing process of fear expression elicited by the preceding threat cue. Moreover, it is not clear whether the lack of effect of the brain stimulation on theta brainwaves was observed because the stimulated region (alPFC) was insufficiently involved in fear processing, or the decreased alPFC activity caused by the stimulation was not captured by brainwaves, or if the effect of cTBS on the brain was too weak.

Introduction

In situations of imminent threat, organisms tend to respond rapidly and adaptively. However, when the threat is no longer present, it is essential to downregulate the fear response back to the baseline. Chronic inability to downregulate the fear response after the disappearance of threat may lead to prolonged anxiety, which could cause a development of anxiety disorders (Etkin & Wager, 2007).

Besides the amygdala, which is confirmed to be involved in fear processing (Méndez-Bértolo et al., 2016), the medial prefrontal cortex (mPFC) has also been found to play a major role in fear expression, fear extinction and fear downregulation (Quirk & Beer, 2006; Fullana et al., 2018). Importantly, the PFC has both excitatory and inhibitory projections onto the amygdala (Barbas, 2000; Milad & Quirk, 2012), which are essential in these processes. The ventromedial PFC (vmPFC) has been found to be involved in fear extinction (Milad et al., 2007), which is supported by studies that have found inhibitory projections from the vmPFC onto the amygdala (Groenewegen et al., 1997; Ghashghaei & Barbas, 2002; Tillman et al., 2018). On the other hand, the dorsomedial PFC (dmPFC) is evidenced to be involved in fear expression (Milad & Quirk, 2012; Chen et al., 2021). Contrary to the vmPFC, the dmPFC has been found to have excitatory projections onto the amygdala which mediate fear expression (Milad & Quirk, 2012).

The important role of the vmPFC in fear extinction and fear downregulation is supported by many neuroimaging studies. Increased vmPFC and decreased amygdala activity have been reported for fear extinguished versus unextinguished stimuli in a 2-day fear conditioning paradigm (Milad et al., 2007). Furthermore, a positive correlation between the rate of fear extinction and the thickness of vmPFC has been reported (Milad et al., 2005), which further confirms the importance of vmPFC in fear extinction.

There is evidence that together with the vmPFC, the anterolateral PFC (alPFC) might also play a role in fear downregulation after threat offset. Klumpers et al. (2010) conducted an fMRI and startle study in which they administered the instructed fear task. In this task, participants were instructed that they will be presented with two different faces. During the presentation of face 1, they might receive an electric shock (threat condition), whereas during the presentation of face 2, they would never receive an electric shock (safe condition). Startle reflex has been evidenced to be an objective and robust measure of the defensive state in humans (Grillon & Baas, 2003). Their results indicate that the defensive state reflected by the startle response was rapidly downregulated within 3.5 seconds after threat offset. Furthermore, their fMRI results suggest that the reduction of the defensive state after threat offset is associated with the concomitant activation of the alPFC (Klumpers et al., 2010). To overcome the correlational nature of fMRI paradigms, a later study conducted in our lab by van Dijk et al. (2017) also administered the instructed fear task and applied repetitive transcranial magnetic stimulation (rTMS) over the alPFC to temporarily decrease the excitability of this region, which allows making causal inferences about the involvement of this area in fear downregulation. Contrary to the original hypothesis of finding increased startle response at threat offset after stimulation, they found a general increase in startle magnitudes both during and after the offset of a threatening stimulus. This might be due to the need to downregulate the general increase of defensive state elicited by the laboratory setting and the possibility of receiving an unpleasant stimulus (Grillon & Ameli, 1998). Therefore, these results indicate that instead of being involved in fear downregulation specifically at threat offset, the alPFC might play a more general role in the downregulation of defensive states.

It has been found that the anterior PFC (aPFC), in which the alPFC is located, is amongst other functions, essential for social emotional action regulation (Bramson et al., 2020). The aPFC-mediated emotion regulation is assumed to happen by downregulating the activity of the

amygdala, which evaluates emotions automatically, and upregulating the activity of regions responsible for deliberate rule selection such as the posterior parietal cortex (Volman et al., 2011; 2013). Furthermore, a recent fMRI and MRI study validated the involvement of alPFC in the regulation of prepotent tendencies evoked by an emotional stimulus by administering the approach-avoidance task (AA). Their connectivity analysis indicates that it is mainly the alPFC that is involved in emotion regulation during the task performance (Bramson et al., 2020). Another reason why this region is a likely candidate for emotion regulation is because of its connections with the amygdala via the amygdalofugal tract (Kamali et al., 2016; Folloni et al., 2019). Bramson et al. (2020) reported that in their data, 10 to 20% of individual differences in emotion regulation could be explained by the strength of the alPFC-amygdala tract.

In addition to neuroimaging studies, fear expression, fear recall, and emotion regulation have also been extensively studied by electrophysiological measures. Converging evidence from animal studies as well as electrophysiological studies in humans indicate that the main mechanism of communication between the PFC and the amygdala in fear behavior is via brain oscillations in the theta range (4-8 Hz) (Karalis et al., 2016; Chen et al., 2021). A recent animal study reported that fear, as expressed through freezing, was most prevalent when oscillations in the theta range (4 Hz) were generated in the PFC-amygdala circuits. Furthermore, their directionality analyses revealed that it was mainly 4 Hz oscillations in the dmPFC that led to the activation of amygdala, and in turn, to freezing (Karalis et al., 2016). This study confirms the importance of theta oscillations generated by the dmPFC in fear expression. These findings have also been translated to human EEG studies (Chen et al., 2021; Sperl et al., 2019).

To confirm that theta is the primary oscillatory mechanism involved in the PFC-amygdala communication during fear processing in humans, Chen et al. (2021) used intracranial EEG recordings from the dmPFC, vmPFC, and amygdala in a fear conditioning paradigm. They reported increased theta power and interregional synchronization of the amygdala, vmPFC, and

dmPFC during the presentation of a conditioned versus unconditioned stimulus. Their analysis of information transfer indicates that during fear conditioning, the activation of the amygdala was driven mainly by the dmPFC, which is in line with the evidence that this region is involved in fear expression (Milad & Quirk, 2012). Furthermore, increased theta power in the frontal areas has been observed when processing threatening visual stimuli (DeLaRosa et al., 2014) and during the presentation of a threat cue in the instructed fear task (Chirumamilla et al., 2019).

Theta oscillations have also been found to play an important role in the recall of fear conditioned stimuli. Mueller et al. (2014) conducted a 2-day experiment, in which the participants completed a differential fear conditioning task, followed by differential fear extinction protocol on day 1, and a fear recall test on day 2. They recorded EEG during the fear recall test and reported increased theta power for unextinguished compared to extinguished stimuli. Furthermore, they source-localized the theta oscillations to the dmPFC. The increased theta during the recall of unextinguished versus extinguished fear conditioned stimulus reflects the process of fear expression, which is generally found to be mediated by the dmPFC (Milad & Quirk, 2012). A follow-up study conducted by Sperl et al. (2019), integrated fMRI and EEG to confirm the involvement of theta oscillations in the communication between the dmPFC and the amygdala. They replicated the previously mentioned results of Mueller et al. (2014) by reporting increased fronto-midline theta power in unextinguished compared to extinguished stimuli. Moreover, they found a strong relationship between theta power and amygdala activity, with theta power explaining 60% of the variation of amygdala activity in fear recall (Sperl et al., 2019). These studies provide substantial evidence that theta oscillations generated by the dmPFC, a region that has been consistently reported to be involved in the expression of fear (Milad & Quirk, 2012; Klumpers et al., 2010), play an important role in fear expression and that they are crucially involved in the communication between the amygdala and the dmPFC (Chen et al., 2021; Sperl et al., 2019).

The literature on the oscillatory processes involved in fear extinction is scarce. Mueller et al. (2014) did not focus directly on the process of fear extinction, but rather the recall of fear extinguished versus unextinguished stimuli. In addition to dmPFC-theta, their study also explored brain oscillations source localized to the vmPFC, a region that is crucially involved in fear extinction (Milad et al., 2005; 2007; Milad & Quirk, 2012) and fear downregulation (Klumpers et al., 2010). They reported increased vmPFC-localized gamma (36.5 – 44 Hz) power in the extinguished versus unextinguished stimuli during the fear recall test. Therefore, they concluded that the recall of unextinguished fear is associated with dmPFC-theta, whereas the recall of fear extinguished stimuli might be related to vmPFC-gamma oscillations (Mueller et al., 2014). Although promising, a follow-up study did not find increased vmPFC-gamma power (30 - 45 Hz) during the recall of successfully extinguished stimuli (Bierwirth et al., 2021). Because of the inconsistent findings, the vmPFC-localized oscillatory processes involved in extinction recall and fear extinction remain unclear.

In addition to fear expression and fear recall, theta oscillations are involved in cognitive control (Cavanagh & Shackman, 2015), motivational behavior (Cavanagh et al., 2013), and emotion regulation (Ertl et al., 2013; Bramson et al., 2018). As mentioned above, the alPFC plays an important role in the regulation of emotional action tendencies (Bramson et al., 2020). A recent MEG study found increased theta power source-localized to the alPFC when participants were selecting an alternative to their prepotent dominant response in a social AA task, in which emotional faces were used as stimuli. This study also reported that reaction time increases in incongruent trials, in which more emotional control needed to be exerted, could be accounted for by the increased alPFC theta power (Bramson et al., 2018). Furthermore, increased power of theta was also observed during cognitive reappraisal, which is a frequently studied emotion regulation technique that instructs participants to reinterpret a negative situation in a way that modifies or reduces the emotional response to the situation (Ertl et al.,

2013). Therefore, the role of theta oscillations might be twofold, the dmPFC theta oscillations are involved in fear expression (Mueller et al., 2014; Chen et al., 2021) while the alPFC theta oscillations are associated with emotion regulation (Bramson et al., 2018; Ertl et al., 2013).

Besides oscillatory mechanisms, there is extensive literature about the late positive potential (LPP), which is a centroparietal event-related potential (ERP) that is sensitive to emotional stimuli (Hajcak & Foti, 2020). LPP begins around 400ms after stimulus onset and is defined as a sustained positive deflection (for a review see MacNamera et al., 2022). LPP has been thoroughly studied in cognitive reappraisal studies which found that as a result of active engagement in cognitive reappraisal, the amplitude of the LPP decreases (Hajcak & Nieuwenhuis, 2006). Furthermore, increased amplitude of LPP has not only been observed during the presentation of emotionally-laden stimuli, but also after the offset of such stimuli. It has been suggested that the attentional capture of emotion persists even after the presentation of an emotional stimulus and that this is reflected by an elevated LPP amplitude (Hajcak & Olvet, 2008).

Aside from emotion regulation, LPP has also been examined in fear processing studies. Larger LPP has been found in fear conditioned (CS+) compared to non-fear conditioned (CS-) trials in a fear conditioning task (Bacigalupo & Luck, 2018) and in an instructed fear task (Gonzalez-Escamilla et al., 2019). Furthermore, Sperl et al. (2021) assessed LPP during different phases of fear conditioning and fear extinction. During fear conditioning, they found that the LPP differences between CS+ and CS- trials were gradually increasing, with CS+ trials having progressively higher LPP amplitudes than CS- trials. Moreover, they reported that the difference in LPP between CS+ and CS- trials gradually decreases from early phase of fear extinction to the late phase of fear extinction. These results are in line with the notion that LPP is an indicator of stimulus significance (Hajcak & Foti, 2020). As the fear conditioning progresses, the significance of the CS+ versus CS- increases, whereas the stimulus significance

gradually decreases during fear extinction (Sperl et al., 2021). Therefore, a robust body of evidence proves that LPP is an adequate measure of the emotional response to the stimulus.

A feasible way of causally studying a brain process is by utilizing the rTMS, which is a non-invasive brain stimulation with the potential to decrease or increase the excitability of cortical brain structures (Lefaucheur et al., 2020). Continuous theta burst stimulation (cTBS) is a commonly chosen rTMS protocol because the duration of stimulation is short (40 seconds) and because it results in a relatively long decrease of cortical excitability (50 minutes) (Wischnewski & Schutter, 2015). A cTBS protocol aimed at inhibiting the aPFC was used in a study conducted by Volman et al. (2011). Participants in this study completed the above-mentioned AA task, and it was found that the cTBS over aPFC led to worse social emotion regulation behavior, as reflected by increased amygdala activity and decreased activity in the aPFC. Authors of this study suggest that the aPFC exerts control over social emotional regulation by coordinating action selection and inhibiting emotionally elicited responses (Volman et al., 2011). This study adds more evidence to the already described involvement of the alPFC in the regulation of emotional behavior (Bramson et al., 2018; 2020; Klumpers et al., 2010).

In our study, we used the instructed fear task similar to the one used by Klumpers et al. (2010; 2012) and identical to the one used by van Dijk et al. (2017). As mentioned above, van Dijk et al. (2017) found increased startle response after active cTBS not only at threat offset, but also during the cue. Our study aims to replicate the startle results and extend them by examining the EEG mechanisms involved in fear expression and fear downregulation and the impact of cTBS over the alPFC on these processes.

For the EEG results we expect to find higher fronto-midline theta power during the presentation of the threat versus safe cue. This is due to the evidence of fronto-midline theta being involved in fear expression (Mueller et al., 2014; Sperl et al., 2019; Chen et al., 2021;

Chirumamilla et al., 2019; Chien et al., 2017). We also expect to find increased theta power in the threat condition compared to the safe condition after the stimulus offset. There are two possible lines of reasoning for this. Increased theta in the threat condition after cue offset might reflect the ongoing fear expression elicited by the stimulus presentation. However, theta oscillations are also involved in emotion regulation (Bramson et al., 2018; Ertl et al, 2013). Therefore, increased theta after the threat versus safe cue offset might also reflect increased emotion regulation responsible for the downregulation of fear. In this case, we expect the topography of theta to closely resemble the alPFC, which has been found to be involved in emotion regulation (Bramson et al., 2018) and fear downregulation (Klumpers et al., 2010). We also expect to observe a higher LPP amplitude in response to the threat stimulus than the safe stimulus because the chance of an upcoming electric shock indicates a higher stimulus significance (Hajcak & Foti, 2020). Furthermore, it has been evidenced that the attentional capture of emotion elicited by the stimulus persists even after the offset of an emotional stimulus (Hajcak & Olvet, 2008). Therefore, we expect to find increased LPP amplitude also after the stimulus offset.

Regarding the TMS manipulation, we expect to find an increase in fronto-midline theta after the active versus control cTBS during the presentation of the threat stimulus. This is because theta oscillations are associated with fear expression (Mueller et al., 2014; Sperl et al., 2019; Chen et al., 2021; Chirumamilla et al., 2019; Chien et al., 2017) and the cTBS-induced inhibition of alPFC, a region involved in emotion regulation (Bramson et al., 2018), will cause a decreased ability to downregulate fear, which will result in a general increase of defensive states (van Dijk et al., 2017). For the cue offset, there are two possibly opposite outcomes. One outcome is in line with the fear expression literature (Mueller et al., 2014; Sperl et al., 2019; Chen et al., 2021; Chirumamilla et al., 2019; Chien et al., 2017). According to this line of thought, the cTBS-induced suppression of alPFC, a region involved in emotion regulation

(Bramson et al., 2018; 2020) and fear downregulation (Klumpers et al., 2010), would cause an increase in fear expression that would persist even after the offset of the threat cue. Therefore, there would be higher fronto-midline theta power post active versus control cTBS after the offset of the threat versus safe cue. On the other hand, theta oscillations are also involved in emotion regulation (Bramson et al., 2018; Ertl et al., 2013). Based on these studies, we would expect to find a decreased power of alPFC-theta especially in the threat condition after active versus control cTBS due to the decreased excitability of the alPFC and therefore, decreased emotion regulation ability mediated by the alPFC-theta oscillations (Bramson et al., 2018). Moreover, because LPP can be viewed as a marker of fear processing (Gonzalez-Escamilla et al., 2019), we expect to find an increase in LPP amplitudes after the active cTBS both during and after the presentation of a threatening stimulus.

Methods

Participants

Based on the outcome of a power analysis, we intended to recruit 30 healthy participants. Our recruitment strategy included distributing flyers and advertising the experiment online. The following attributes were used as the exclusion criteria for our study: history of, or current neurological or psychiatric illness, extensive medical history, alcohol or drug abuse in the past 6 months and other TMS contraindications (Keel et al., 2001) that include history of closed or open head injury, and ferrous objects in or around the head. Furthermore, all participants were right-handed (assessed by the Edinburgh Handedness Inventory, Dragovic, 2004) and between 18 and 45 years of age. All participants signed the informed consent form. The study was approved by the medical-ethical committee of Utrecht University and all subjects received compensation of €8 per hour.

Instructed fear task

In total, participants completed this task four times, two times on each session. The instructed fear task was adapted from Klumpers et al. (2010, 2012) and was identical to the one used by van Dijk et al. (2017). In this task, pictures of emotionally neutral male faces with either blue or orange background, which served as cues, were presented. At the beginning of the task, participants were instructed that one of the cues is associated with the possibility of receiving an electric shock (threat cue), whereas no shock will be presented in the other cue (safe cue).

The electric shocks were administered through a current stimulator (Digitimer DS7A, Digitimer Ltd), which was connected to tin cup electrodes that were placed on the median nerve of the left wrist. To establish the shock intensity that would be rated as "quite annoying", participants completed a shock work-up procedure that took place prior to the instructed fear task (Klumpers et al., 2010). In the shock work-up, participants initially received mild electric shock, and the intensity of the shock increased or decreased based on their rating of the shock on a 5-point Likert scale (with the intention of achieving a 4 out of 5 rating). This intensity was then used throughout the whole instructed fear task.

During the second time participants competed this task on each session, the cues were presented in a reversed order to prevent the predictability of receiving the shock. Furthermore, the association of which cue was paired with the electric shock was counterbalanced across participants. After the presentation of the instructions, the startle habituation phase began. The initial startle habituation before the first block consisted of 8 startle probes and 2 startle probes were presented before the subsequent blocks. The first two blocks consisted of 40 trials (20 per condition) in a semi-random order, which lasted for 4-8 s (M = 5.6 s). Each trial was followed by a 6-20.5 s (M = 11.2 s) rest period that was instructed by "RUST" (Dutch for "rest") presented on the screen. The third block consisted of 20 trials, resulting in 100 trials in total (50 per condition). The shock during the threat cue was administered 9 times in total (Table 1). All

blocks were followed by Visual Analogue Scales (VAS) in which participants were asked to rate their level of fear in response to both conditions as cued by the different faces. The scale ranged from "not anxious/nervous" to "very anxious/nervous".

Startle

The startle probes were delivered binaurally through in-ear earplugs (Earlink, IN, USA). Startle was probed by a 50 ms 106 dB white noise bursts that have been found to consistently evoke a startle response (Grillon & Baas, 2003). Besides habituation, the startle responses were probed either during the cue presentation (3 s post-cue-onset), or after cue offset (1.5 s post-cue-offset or 5 s post-cue-offset) (Table 1).

Table 1. *The amounts of trials per condition and the amounts of startle probes and shocks administered during the task*

	Block	*1*	*2*	*3*	*Total*
		VAS + hab	*VAS + hab*	*VAS + hab* *VAS*	
Cue	Threat	20	20	10	50
	Safe	20	20	10	50
Startle probe	Threat cue	8	8	4	20
	Safe cue	8	8	4	20
	Threat offset $_{\text{early + late}}$	4+4	4+4	2+2	20
	Safe offset $_{\text{early + late}}$	4+4	4+4	2+2	20
	Shock	4	4	1	9
Time (min)		11.1	11.1	5.6	27.8

TMS machine, motor threshold determination, cTBS practice session and cTBS

The TMS setup consisted of a Magstim Rapid Stimulator (Magstim Company Ltd, Whitland, UK) with a figure-of-eight coil consisting of 92mm diameter AirFilm – Rapid version.

The motor threshold determination procedure that we used was developed and validated by Schutter & van Honk, (2006). In this procedure, single TMS pulses are applied on the left primary motor cortex of participants as localized by the EEG cap (C3 electrode). The active motor threshold (AMT) is the stimulation intensity that produces a motor evoked potential

(MEP) in 5 out of 10 trials. We used the staircase procedure, in which the machine stimulation intensity starts at 50% and gradually increases by 2% if no MEP is evoked in 50% of given pulses or decreases by 5% if the MEP is evoked in more than 50% of given pulses. The success of evoking the motor potential was determined by visual observation of the right hand by two administrators of the experiment.

After the motor threshold determination participants underwent a cTBS practice session to be familiarized with the cTBS procedure. In this session, they received 3 seconds of cTBS (45 pulses at 15 Hz) on both the active (alPFC, between the electrodes AF4 & Fp2) and the control stimulation site (vertex, electrode Cz). After the practice session participants could decide if they wanted to proceed with the experiment.

The cTBS protocol consists of bursts of 3 pulses at 50 Hz repeated every 200 ms lasting for 40 s resulting in 600 pulses in total. To improve the stability of the coil placement, a cotton pad was attached to the midpoint of the coil. On each session, subjects received either active or control cTBS with the machine output equal to 80% of their AMT. The order of stimulation type was counterbalanced across participants.

Subjective measures

Multiple types of subjective measures were digitally recorded. The fearfulness ratings during the onset and the offset of both cues were assessed by the VAS after the end of each block. Furthermore, the State-Trait Anxiety Inventory (STAI) was used to assess trait and state anxiety (Spielberger et al., 1970; van der Ploeg & Defares, 1980). The STAI-state was completed 2 times during each session. The STAI-trait was filled out once, at the beginning of the first test day.

Procedure

Before scheduling the first session, participants were asked to read a list of all exclusion and inclusion criteria, together with a detailed information letter and confirm that they meet the criteria and are willing to participate. After arrival for the first session, participants filled out a short battery of questionnaires, including the checklist with inclusion and exclusion criteria. Next, we determined their motor threshold and completed a short TMS practice session after which participants could decide if they want to continue the experiment. Then, participants filled out both subsets of the STAI (Spielberger et al., 1970; van der Ploeg & Defares, 1980). These steps took about 30 minutes and were only done on the first session, while the following steps were completed on both sessions. Then, the shock electrodes were attached and the shock work-up was performed to establish the shock intensity for the instructed fear task. Afterwards, the EEG, EMG, and skin conductance electrodes were attached, and participants completed the instructed fear task for the first time. After that, all electrodes were disconnected from the amplifier, participants moved to a different chair, and active or control cTBS was administered. Then the electrodes were reconnected, and participants completed the instructed fear task for the second time. Before the end of the session, participants filled out the STAI-state and a short TMS aversiveness questionnaire (Figure 1). In total, the first session took around 2.5 hours, and the second session took around 2 hours. The sessions were separated by around one week (M = 7.3 days, SD = 1.75).

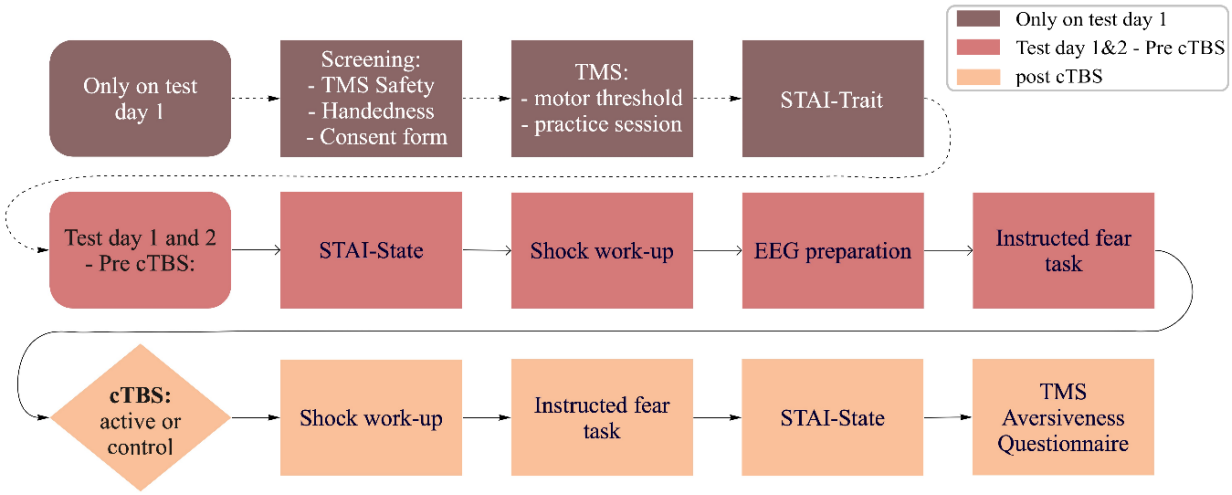

Figure 1. *The sequence of the experimental procedure*

EEG apparatus

In this study, the 64-channel BioSemi Active-Two amplifier system (Biosemi, Amsterdam, the Netherlands) was used and the electrodes were positioned in accordance with the 10/20 system. Additionally, seven external electrodes were used. For the vertical electrooculogram (VEOG), the electrodes were placed above and below the right eye and for the horizontal electrooculogram (HEOG) the electrodes were placed on the outer canthi of each eye. External electrodes were also placed on the mastoid on both sides. Furthermore, next to the VEOG electrode below the eye, there was one extra 15 mm laterally placed electrode for the startle measurement (Blumenthal et al., 2005). The sampling rate of 2048 Hz was used for recording the data and the electrode offsets were kept in the -20 mV to 20 mV range.

Data analysis

EEG preprocessing

EEG was processed offline using the BrainVision Analyzer Version 2.1 (Brain Products GmbH, Gilching, Germany). First, data was downsampled to 256 Hz, re-referenced to the average of mastoid electrodes, filtered (low cutoff: 0.5 Hz, high cutoff: 30 Hz) and segmented based on the condition (stimulus Onset or Offset, Threat or Safe). Then, artifact rejection and

ocular correction were performed (Gratton, Coles & Donchin, 1983). Afterwards, the artifact rejection was conducted again to remove any residual artifacts that were not corrected in the previous step. The following criteria were applied for the second artifact rejection: maximal allowed voltage step: 50 μV/ms, maximal allowed difference of values: 200 μV, minimal/maximal allowed amplitude: -200 μV, 200 μV respectively, lowest allowed activity: 0.5 μV in 100ms. After the artifact rejection, 2 participants were left with an insufficient number of trials and therefore were excluded. This left us with a total sample of N=28. For the visualization of the data, all cue onset segments that contained a startle probe or an electric shock were excluded. Those cue-offset trials that contained an early startle probe or an electric shock during the trial were excluded as well. Moreover, for all the subsequent transformations and analyses, only the trials without startle probes or electric shocks in the defined time window of interest were included in averaging.

Wavelet transforms

At first, -1500ms to 5000ms segments were made. Then, a continuous complex Morlet wavelet transformation was performed with the baseline of -500 to -200ms before the cue onset for the onset data and -500 to -200ms before the cue offset for the offset data. To cut out the edge artifacts (Cohen, 2014), the data was re-segmented to -500 to 4000ms and averaged for each condition. To identify the frequency bands that differed from the baseline, we first computed the Wavelet transform for the 1 to 30 Hz frequency range with a 30-step logarithmic resolution. After identifying the frequency ranges of interest, separate wavelet transforms were computed for the specified frequency ranges of interest to ensure that the extracted data will precisely represent the identified frequency range due to the choice of logarithmic frequency steps. To normalize the data, percentage change was calculated (100% = the power at the baseline).

LPP

For the data preprocessing aimed at the extraction of LPP, segments of -200 to 4000ms were made. Furthermore, the pre-stimulus interval (-200 to 0ms) was used for baseline correction.

Post-hoc exploratory analysis of the impact of cTBS on brain oscillations: Resting state data

In addition to investigating the impact of cTBS on brain oscillations during the instructed fear task, we also conducted a post-hoc exploratory analysis on the effects of cTBS on resting state brain oscillations. At the beginning of the instructed fear task, there was a startle habituation period. A four second period around the startle probe was excluded and the rest of the habituation phase was used as resting state data. This data was recorded within 5 minutes post-cTBS. Furthermore, to explore the development of the cTBS effects on brain oscillations in time, the 1.75 to 5.75 second periods after cue offset, in which participants are instructed to rest, were divided into 4 chronological quarters, and were used for analysis. The data was segmented into 2-second-long segments and Fast Fourier Transform was used to transform the data to power density (μV^2/Hz). The frequency bands: delta (0.5 to 4 Hz), theta (4 to 8 Hz), alpha (8 to 12 Hz), and beta (12 to 30 Hz) were exported from the pooled AF4 & Fp2 electrodes (alPFC) and used for analyses. These electrodes were selected for this analysis because they were used as cTBS site and therefore should have the highest sensitivity to cTBS-related changes.

Analysis strategy

Identification of the Frequency-Time-Electrode of Interest (FTE-OI):

Identification of the FTE-OI was performed on the grand averaged data across all conditions. At first, we visually inspected the 1 to 30 Hz frequency range and identified frequency bands that recorded a difference from the baseline in response to cue onset or offset (Figure 2). After identifying the frequency bands of interest, separate wavelet transforms were

computed for each frequency band of interest. To identify the time window with the highest power increase in each frequency band of interest, we extracted, averaged, and plotted all layers of the wavelet. These plots show the averaged power for the defined frequency band of interest on the Y axis and time on the X axis (Figure 3, 4A, 5A, 8A, 9A). Based on these plots we were able to identify the latency of the peak with the highest power increase and select a time window that encompasses the power increase with the largest magnitude. A priori considerations suggest that our analyses should be focused on fronto-midline electrodes, with the probable source in dmPFC (Fz electrode in: Mueller et al., 2014; Sperl et al., 2019) and pooled AF4 and Fp2 electrodes that anatomically correspond with the alPFC (Bramson et al., 2018). Therefore, the fronto-midline electrode with the highest power increase was selected for analysis, whereas the pooled AF4 and Fp2 electrodes were also always selected. The identified FTE-OI was exported and used for statistical analysis.

Statistical analysis

This study used a single-blinded within-subject design. The extracted data from the identified FTE-OI was analyzed by using repeated measures analyses of variance (RMANOVA). At first, a 3-way RMANOVA with the factors 'cTBS' (Active/Control), 'Pre/Post' (stimulation phase) x 'Threat/Safe' (cue condition) was carried out separately for the cue onset and offset data and separately for the fronto-medial and alPFC data. Furthermore, we did not find systematic differences between the active and control pre-cTBS data, which means there are no pre-cTBS differences to correct for. Therefore, because of our specific interest in the effect of cTBS and the fact that the pre-stimulation data may add its own source of noise to the analysis, we also conducted a 2x2 (cTBS, Threat/Safe) RMANOVA only on the post-stimulation data separately for cue onset and cue offset and separately for fronto-medial and alPFC data. All analyses were conducted in SPSS 28 (IBM Cor., Armonk, N.Y. USA). In the following section the outcomes of the statistical analyses related to our hypotheses (main effects

and interactions of the factors Threat/Safe and cTBS) are described. A detailed report with the results for all the factors can be found in Table 2 and Table 3.

Results

Research Sample

In total, we recruited 34 participants, however, 4 participants did not finish the experiment and therefore the total sample for data processing consisted of 30 participants (M age = 23.57, SD = 3.65, 16 female). After EEG preprocessing, 2 additional participants were excluded due to a high number of artifacts, leaving the total sample for statistical analysis N = 28 (M = 23.36, SD = 3.63, 15 female).

Startle, subjective data, skin conductance

The results of the statistical analyses of these measures are described in Rodenburg et al. (2022). This thesis focuses on the EEG part of this project.

Overall identification of the frequencies of interest

To identify the frequency bands with the largest changes in response to the cue onset and offset compared to the baseline, a grand average for the wavelet transform of 1 to 30 Hz across all participants and conditions was produced for cue onset (Fig. 2a) and cue offset data separately (Fig. 2b).

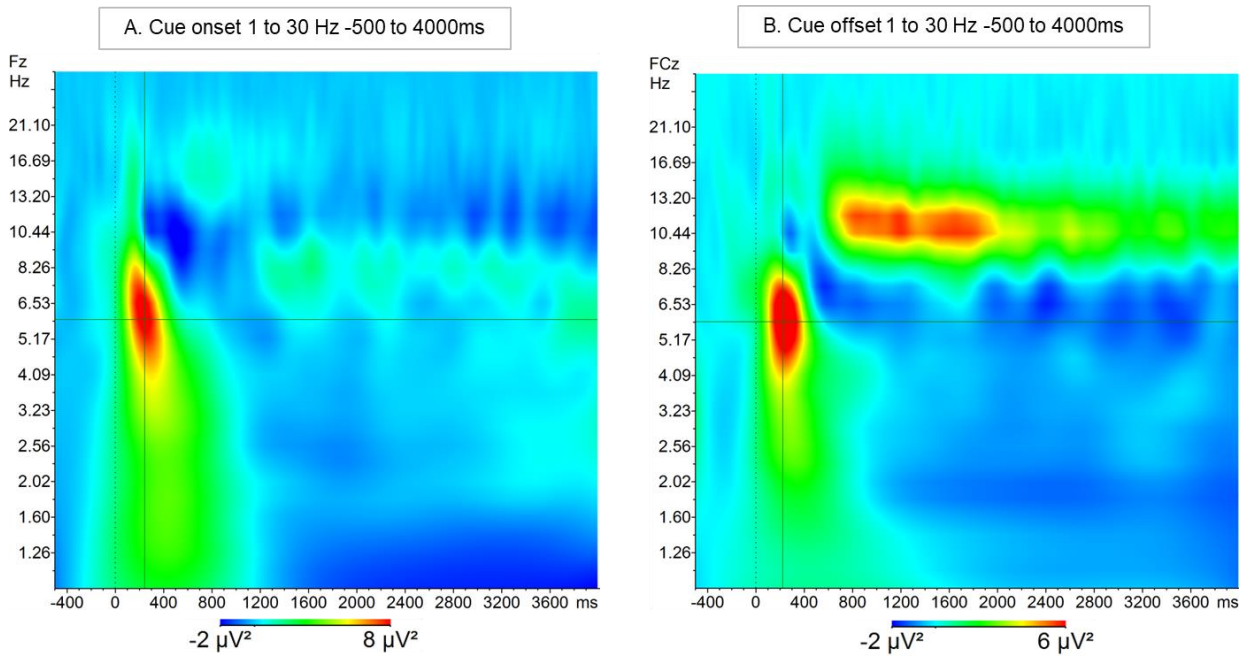

Figure 2. *Grand averages of the wavelet transforms: 1 to 30 Hz scaled logarithmically. Averaged across all conditions (cTBS, Pre/Post, Threat/Safe) and participants. A. Cue onset, electrode: Fz, B. Cue offset, electrode FCz*

For the cue onset, the main oscillatory bands that differed from the baseline were in the theta (4 to 8 Hz) and delta (0.5 to 4 Hz) range. For the cue offset, there was an increase in theta, delta, and alpha (9 to 13 Hz) band.

Theta oscillations

Cue onset: Identification of the electrode and the time window of interest

For cue onset, theta power was increased fronto-medially and the Fz electrode was chosen for analysis (Figure 3B). The same electrode was analyzed in other fear expression studies (Mueller et al., 2014; Sperl et al., 2019). Furthermore, due to the specific interest in the alPFC-theta, pooled AF4 & Fp2 electrodes were chosen for analysis (Figure 3B). In both electrode sites, we selected the time window of 50 to 450ms because it recorded the highest increase of theta power (Figure 3A).

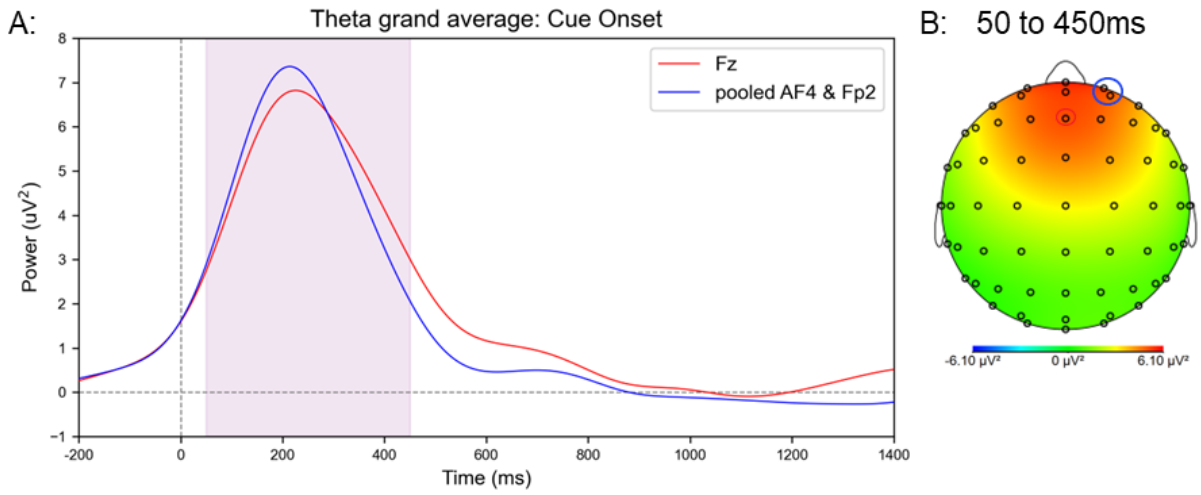

Figure 3. *Extracted and averaged wavelet layers for the whole theta range (4 to 8 Hz) in response to cue onset across conditions (Pre/Post, cTBS, Threat/Safe) and the topography for the selected time window. A: Grand average of theta power for cue onset: selected time window = 50 to 450ms. B: topography for cue onset in the selected time window.*

Cue onset: Statistical analysis

Against our hypotheses, the 3-way RMANOVA revealed no main effect of cTBS ($p > 0.1$) or Threat/Safe ($p > 0.1$). Furthermore, the analysis showed that neither of these factors interacted with other factors ($p > 0.1$). Statistically non-significant results were also obtained for a wide array of electrodes (Fp1, Fpz, Fp2, AF3, AFz, AF4, F1, Fz, F2, FC1, FCz, FC2, C1, Cz, C2) that were analyzed post-hoc to explore the source of theta (Appendix 1).

Cue offset: Identification of the electrode and the time window of interest

For the cue offset, the highest power increase was observed around the FCz electrode in the same time window as for cue onset (50 to 450ms) (Figure 4A, C). In the pooled AF4 & Fp2 electrodes, the power increase was of a lesser intensity and peaked slightly later than in the FCz electrode, therefore, the time window of 100 to 575ms was selected (Figure 4A, B).

Cue offset: Statistical analysis

The 3-way RMANOVA showed a significant main effect of the Threat/Safe factor in both fronto-midline ($F_{(1,27)} = 16.257$, $p < 0.001$, Figure 4D, H, E) and alPFC ($F_{(1,27)} = 6.547$, $p = 0.016$, Figure 4D, G, F) electrode sites. In line with our hypothesis, theta percentage change was higher in the threat condition (fronto-midline: M = 142.197, alPFC: M = 133.014) than in the safe condition (fronto-midline: M = 123.082, alPFC: M = 121.714). There was no main effect or interaction of the cTBS factor ($p > 0.1$, Table 2).

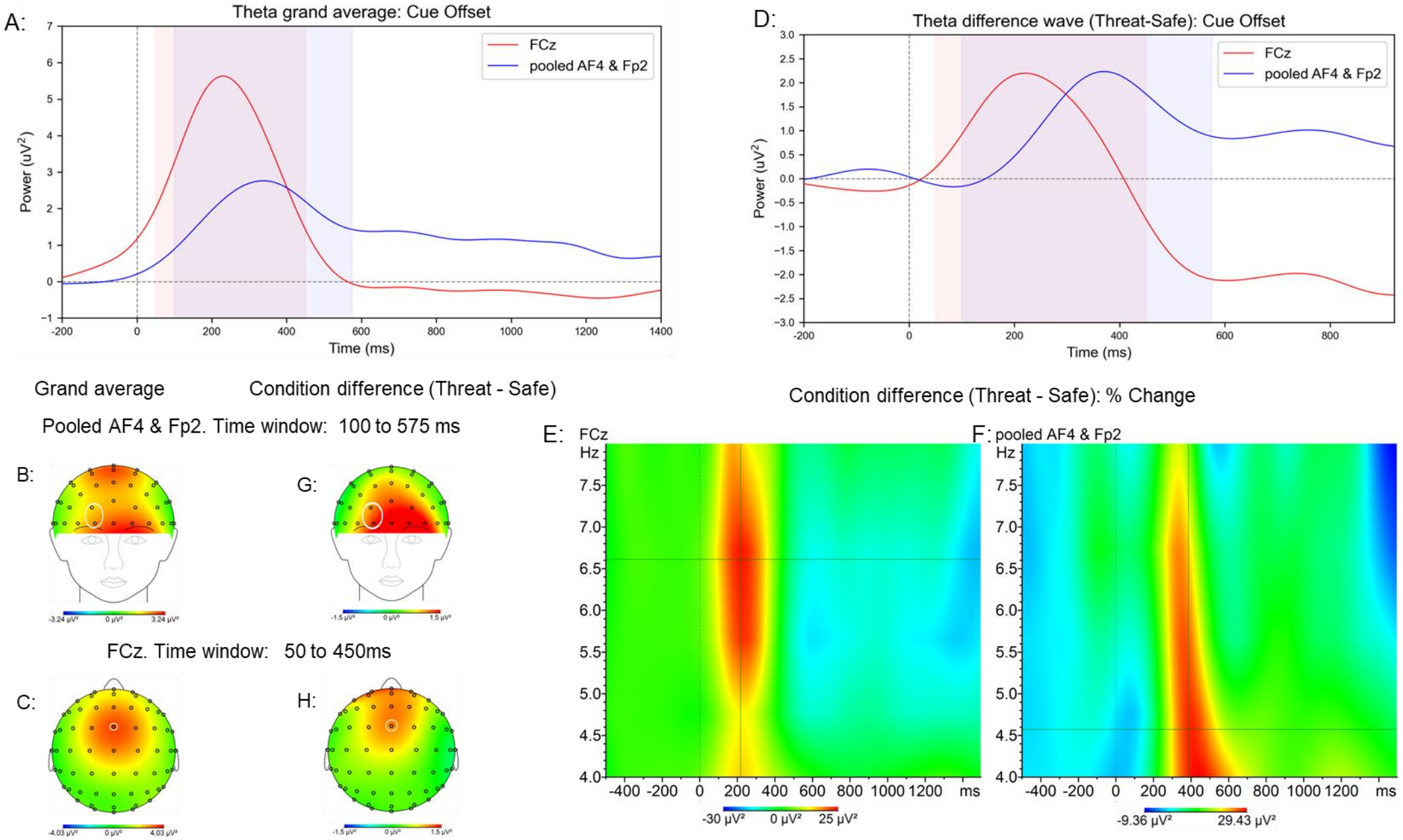

Figure 4. *Theta after cue offset. Line plots (A, D) = Extracted and averaged wavelet layers for the whole theta range (4 to 8 Hz). A, B, C = Grand Averaged data across conditions (Pre/post, cTBS, Threat/Safe). D, G, H, E, F = Condition differences (Threat - Safe). A. selected time window: FCz = 50 to 450ms, pooled AF4 & Fp2 = 100 to 575ms. B. alPFC grand average topography. C. FCz grand average topography. D. Theta difference wave. E. Heatmap for the condition difference in the FCz electrode. F. Heatmap for the condition difference in the pooled AF4 & Fp2 electrodes. G. alPFC topography for the condition differences. H. FCz topography for the condition differences.*

Delta oscillations

Cue onset: Identification of the electrode and the time window of interest

For the cue onset, a fronto-midline increase similar to the one observed in theta oscillations was also observed in the delta range (Figure 5A, B). However, for delta oscillation, this increase was more anterior (Figure 5B). Both the electrode Fz and pooled AF4 & Fp2 recorded a similar increase in delta power during the cue onset and were chosen for statistical analysis. The highest increase was observed in the 50 to 900ms time window for both electrode sites (Figure 5A).

Cue onset: Statistical analysis

The 3-way RMANOVA for the fronto-midline delta revealed a statistically significant main effect of Threat/Safe ($F_{(1,27)} = 4.463$, $p = 0.044$). Higher delta power was observed in the threat condition (M = 127.079) than in the safe condition (M = 122.521) (Figure 5, C, D, E). This effect was absent in the alPFC electrodes ($p > 0.1$, Table 2). Furthermore, delta range was the only frequency band that captured a statistically significant interaction of cTBS with Pre/Post. This interaction was present in both electrode sites (fonto-midline: $F_{(1,27)} = 4.916$, $p = 0.035$, alPFC: $F_{(1,27)} = 4.722$, $p = 0.039$). A further 2x2 (cTBS x Threat/Safe) RMANOVA revealed that it was the post-stimulation data that was driving the interaction. This analysis showed a significant main effect of cTBS for the alPFC delta ($F_{(1,27)} = 6.608$, $p = 0.016$, Figure 6) and a trend level for the main effect of cTBS for the fronto-midline delta ($F_{(1,27)}= 3.787$, $p = 0.062$, Figure 6). Delta power was lower after active cTBS than control cTBS in both fronto-midline delta (Active: M = 120.439, Control: M = 125.476) and alPFC delta (Active: M = 120.908, Control: M = 128.678) (Figure 6). In both cases, the factor cTBS did not interact with Threat/Safe ($F < 1$, Figure 7) meaning that the delta power decrease post-active cTBS did not depend on the cue condition.

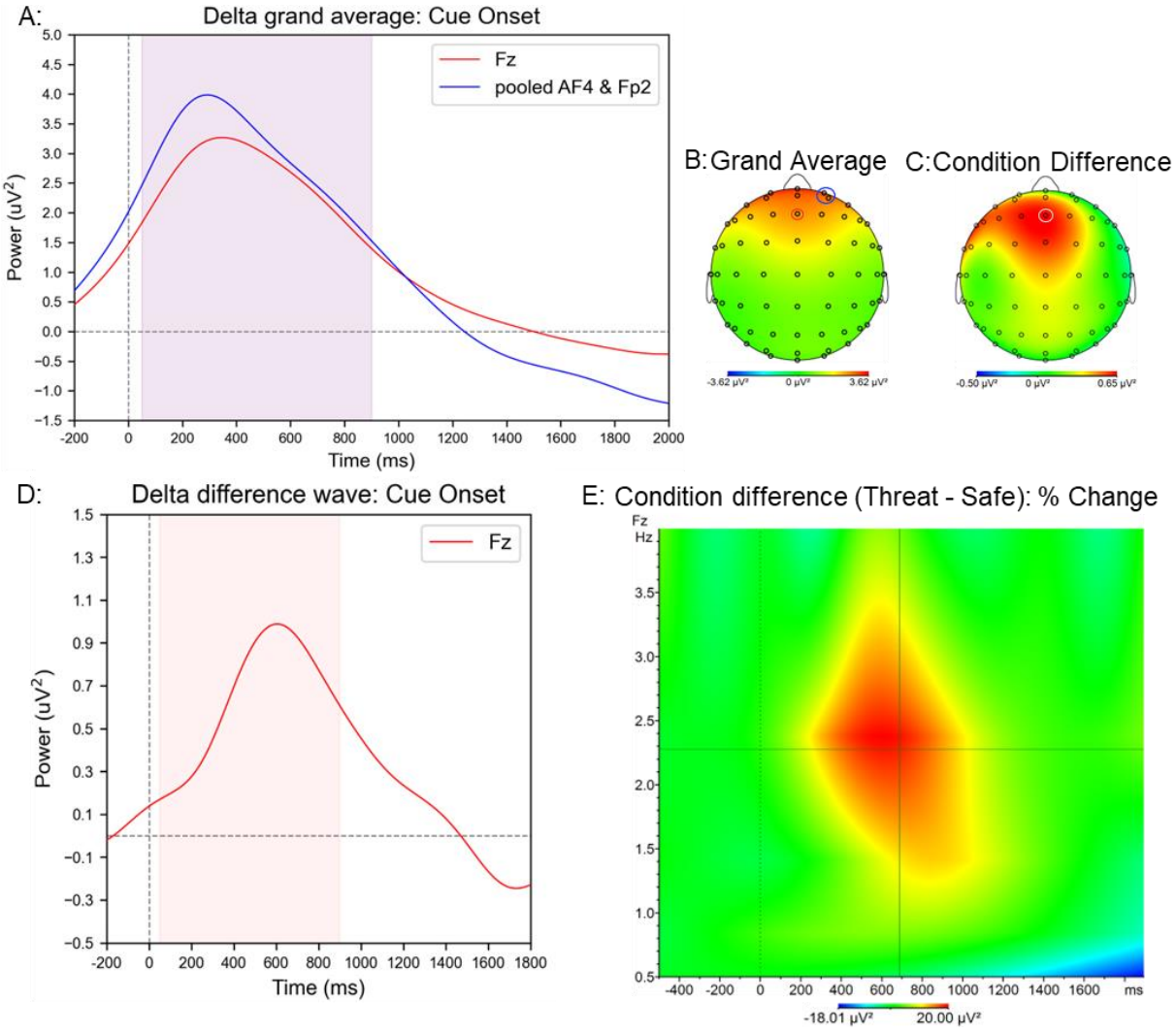

Figure 5. *Delta after cue onset. Line plots (A, D) = Extracted and averaged wavelet layers for the whole theta range (4 to 8 Hz). A, B = Grand Averaged data across conditions (Pre/post, cTBS, Threat/Safe). C, D, E = Condition differences (Threat - Safe). A. selected time window: 50 to 900ms for both electrode sites. B. grand average topography. C. Difference topography. D. Delta difference wave. E. Heatmap for the condition difference in the Fz electrode.*

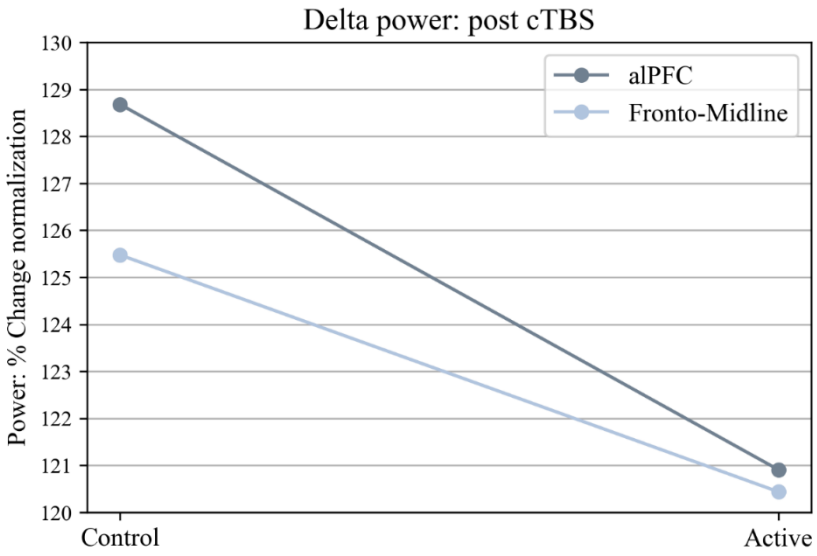

Figure 6. *Delta power decreased after active versus control cTBS.*

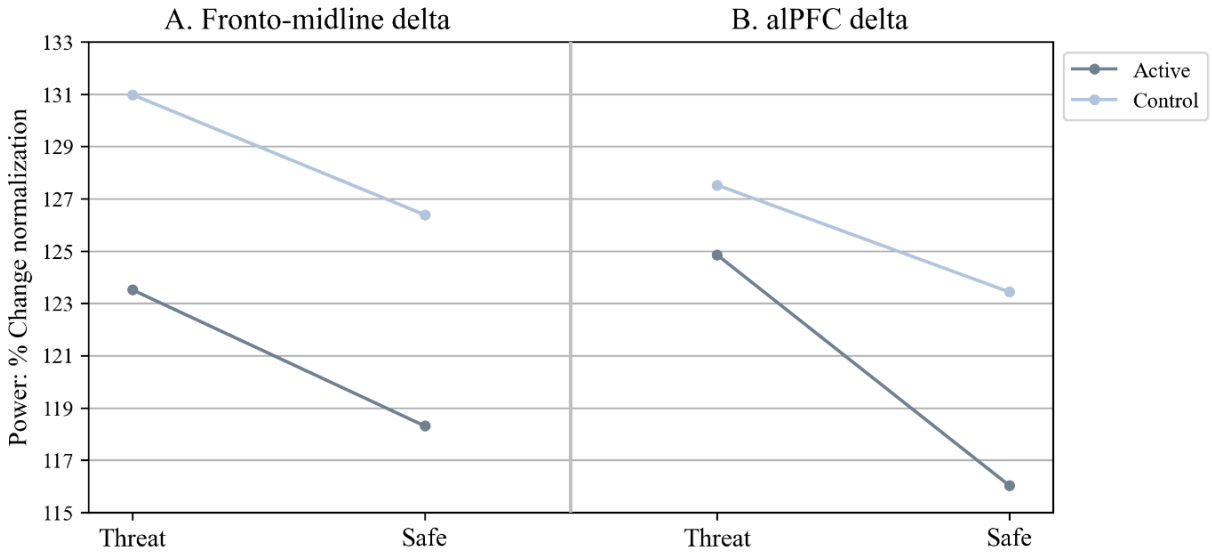

Figure 7. *The absence of an interaction of cTBS with Threat/Safe. cTBS caused a general decrease of delta power in both threat and safe conditions after active cTBS.*

Cue offset: Identification of the electrode and the time window of interest

After the cue offset, the highest power increase was observed frontally in the pooled AF4 & Fp2 (Figure 8A, B). An increase of lesser intensity was also observed in the Fz electrode (Figure 8A, C). To keep the analyses consistent, delta power from both electrode sites was selected. For the Fz electrode, the time window of 100 to 950ms recorded the highest power

increase. The peak of the power increase for the pooled AF4 & Fp2 occurred slightly later and therefore a time window of 200 to 1200ms was selected (Figure 8A).

Cue offset: Statistical analysis

The 3-way RMANOVA also revealed a significant main effect of Threat/Safe in both fronto-medial ($F_{(1,27)} = 25.244$, $p < 0.001$, Figure 8D, H, E) alPFC electrode sites ($F_{(1,27)} = 14.991$, $p < 0.001$, Figure 8D, G, F). Like in theta band, the percentage change of delta was also higher in the threat condition (fronto-medial: M = 121.146, alPFC: M = 135.185) than in the safe condition (fronto-medial: M = 112.347, alPFC: M = 118.768). For delta cue offset data, there was no main effect or interaction of cTBS ($p > 0.1$, Table 2).

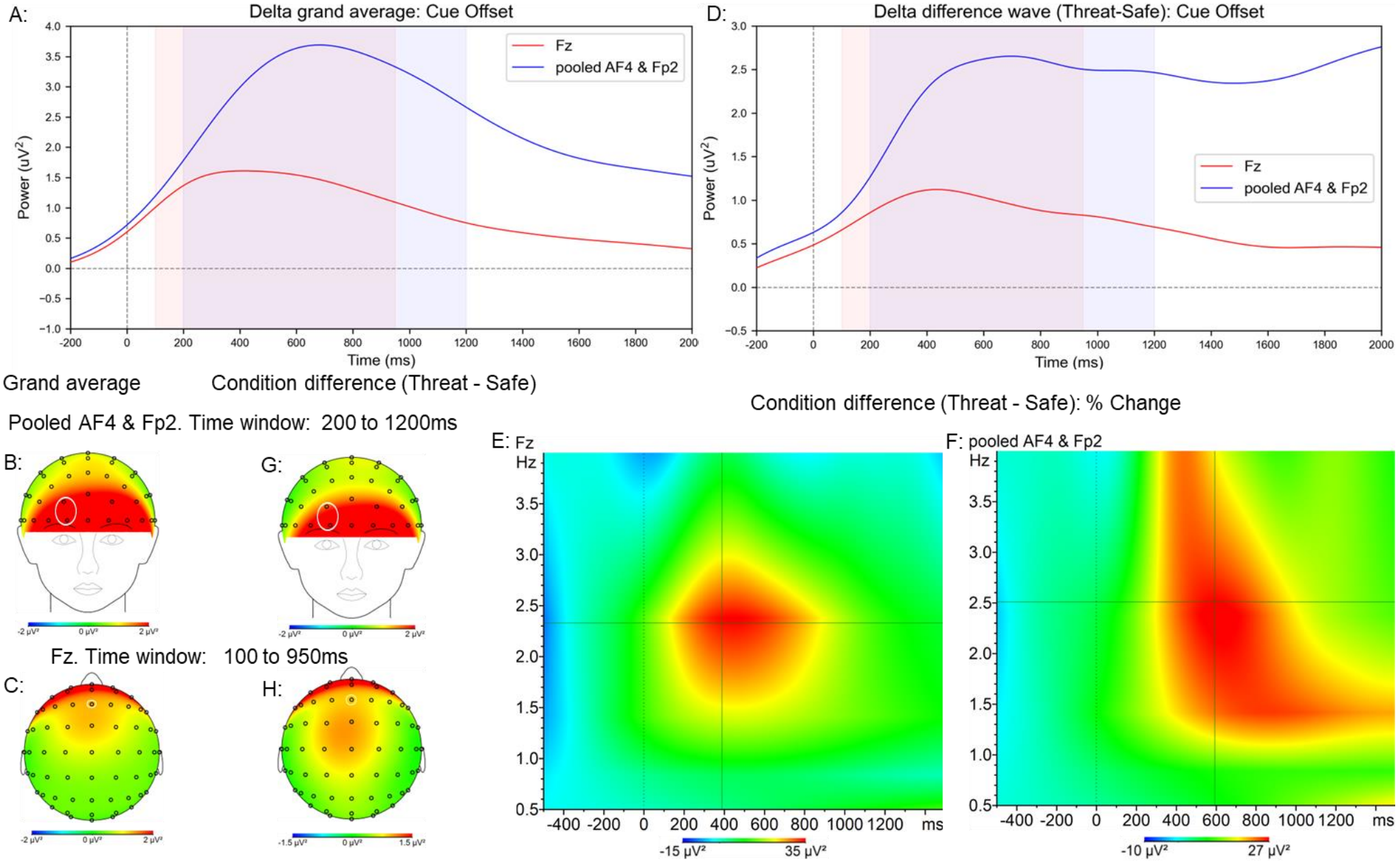

Figure 8. *Delta after cue offset. Line plots (A, D) = Extracted and averaged wavelet layers for the whole delta range (0.5 to 4 Hz). A, B, C = Grand Averaged data across conditions (Pre/post, cTBS, Threat/Safe). D, G, H, E, F = Condition differences (Threat - Safe). A. selected time window: Fz = 100 to 950ms, pooled AF4 & Fp2 = 200 to 1200ms. B. alPFC grand average topography. C. Fz grand average topography. D. Delta difference wave. E. Heatmap for the condition difference in the Fz electrode. F. Heatmap for the condition difference in the pooled AF4 & Fp2 electrodes. G. alPFC topography for the condition differences. H. Fz topography for the condition differences.*

Alpha oscillations

Cue offset: Identification of the electrode and the time window of interest

Increased alpha power was observed only after cue offset. Alpha power increase was observed in two areas: frontally and posteriorly (Figure 9B). For the frontal increase, the Fz electrode was selected, whereas pooled PO4, PO8, and O2 electrodes were selected for the posterior increase (Figure 9B). For both electrode sites, the highest power increase was observed in the same time window: 650 to 2150ms (Figure 9A).

Cue offset: Statistical analysis

The 3-way RMANOVA for alpha oscillations also revealed a significant main effect of Threat/Safe after cue offset at both Fz electrode ($F_{(1,27)} = 5.619$, $p = 0.025$, Figure 9C, D, E) and pooled PO4, PO8, O2 electrodes ($F_{(1,27)} = 12.292$, $p = 0.002$, Figure 9C, D, F). Alpha percentage change was higher in the threat condition (Fz: M = 132.563, pooled PO4, PO8, O2: M = 179.217) than in the safe condition (Fz: M = 123.271, pooled PO4, PO8, O2: M = 151.059). We observed no main effect or interaction of the cTBS factor ($p > 0.1$, Table 2).

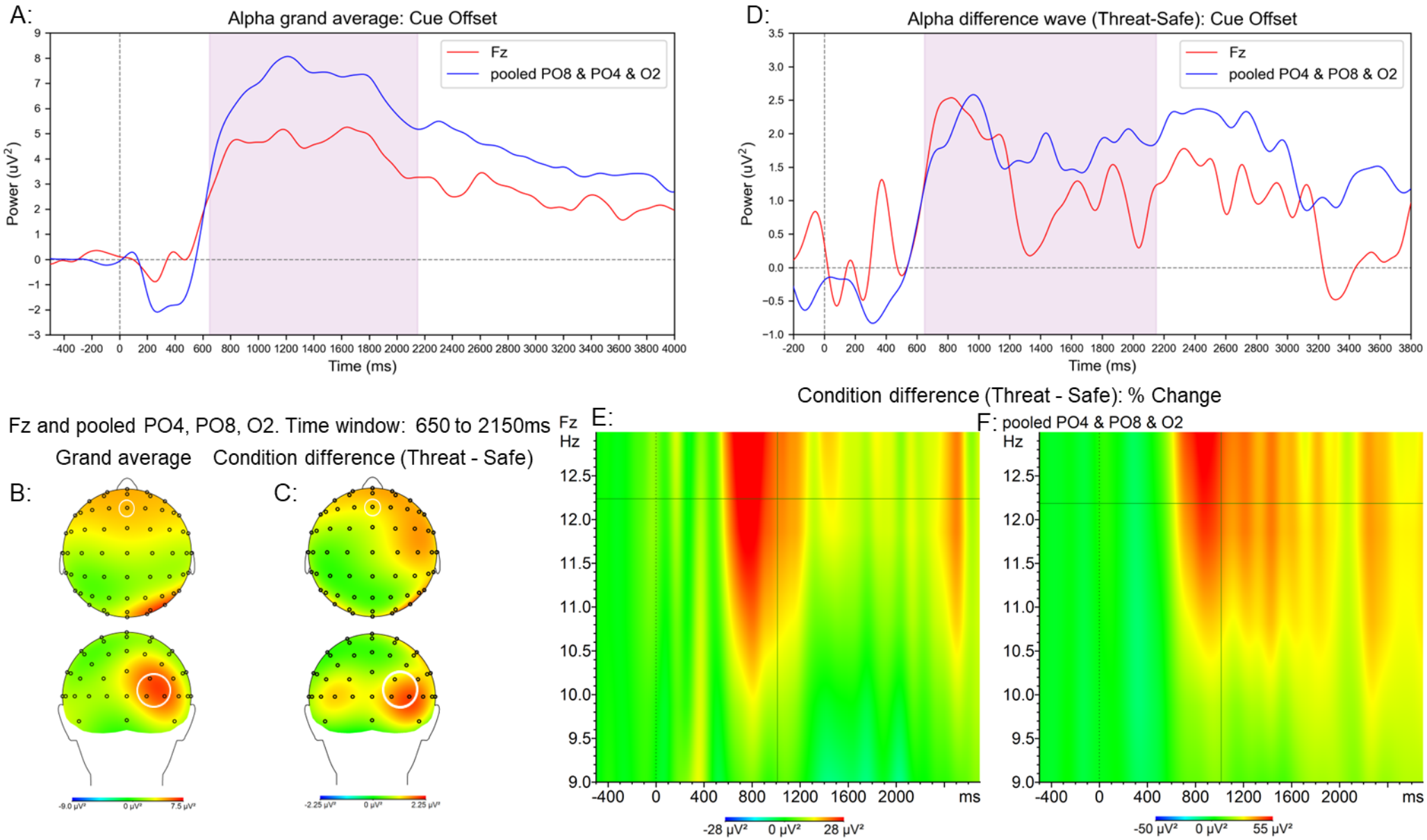

Figure 9. *Alpha after cue offset. Line plots (A, D) = Extracted and averaged wavelet layers for the whole alpha range (9 to 13 Hz). A, B = Grand Averaged data across conditions (Pre/post, cTBS, Threat/Safe). C, D, E, F = Condition differences (Threat - Safe). A. Selected time window 650 to 2150ms. B. Grand average topography: top: Fz circled, bottom: pooled PO4, PO8, O2 circled. C. Condition difference topography: top: Fz circled, bottom: pooled PO4, PO8, O2 circled. D. Alpha difference wave. E. Heatmap for the condition difference in the Fz electrode. F. Heatmap for the condition difference in the pooled PO4, PO8, O2 electrodes.*

LPP

Cue onset: Identification of the electrode and the time window of interest

Based on visual inspection of the grand averaged waveform (Figure 10) and previous literature on LPP (Hajcak & Nieuwenhuis, 2006; Bacigalupo & Luck, 2018; Gonzalez-Escamilla et al., 2019; MacNamera et al., 2019), the time window of 400 to 1000ms was selected for the early LPP and 1000 to 3000ms time window was selected for the late LPP. The highest increase was observed in the pooled POz, PO3, PO4 electrodes and therefore these electrodes were selected for statistical analysis (Figure 10).

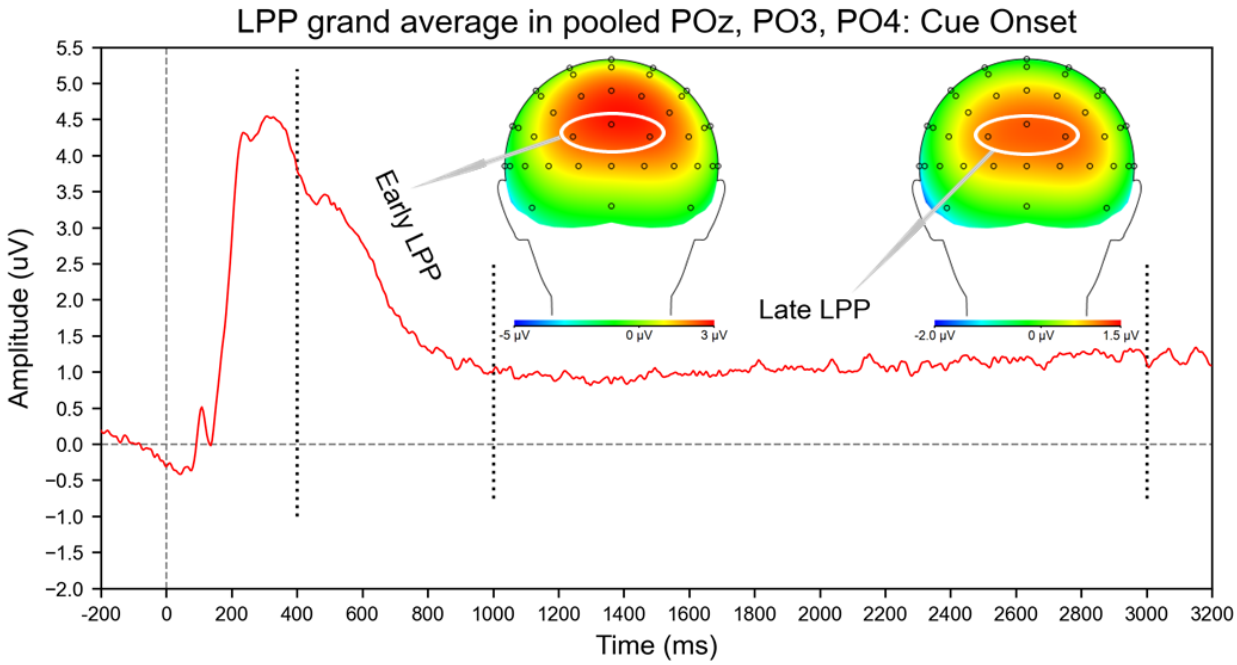

Figure 10. *LPP after cue onset: Grand Average (Pre/post, cTBS, Threat/Safe). Early LPP: 400 to 1000ms, Late LPP: 1000 to 3000ms.*

Cue onset: Statistical analysis

As expected, a 3-way RMANOVA revealed a significantly higher amplitude of early LPP in the threat condition (M = 2.606µV) than in the safe condition (M = 1.608µV) (main effect of Threat/Safe: $F_{(1,27)} = 53.735$, $p < 0.001$, Figure 11). Similarly, the late LPP also showed higher amplitude in the threat condition (M = 1.193µV) than the safe condition (M = 0.928µV)

($F_{(1,27)}$ = 13.681 p < 0.001, Figure 11). Furthermore, the 3-way RMANOVA showed no main effect or interaction of cTBS for both early and late LPP (p > 0.1, Table 3).

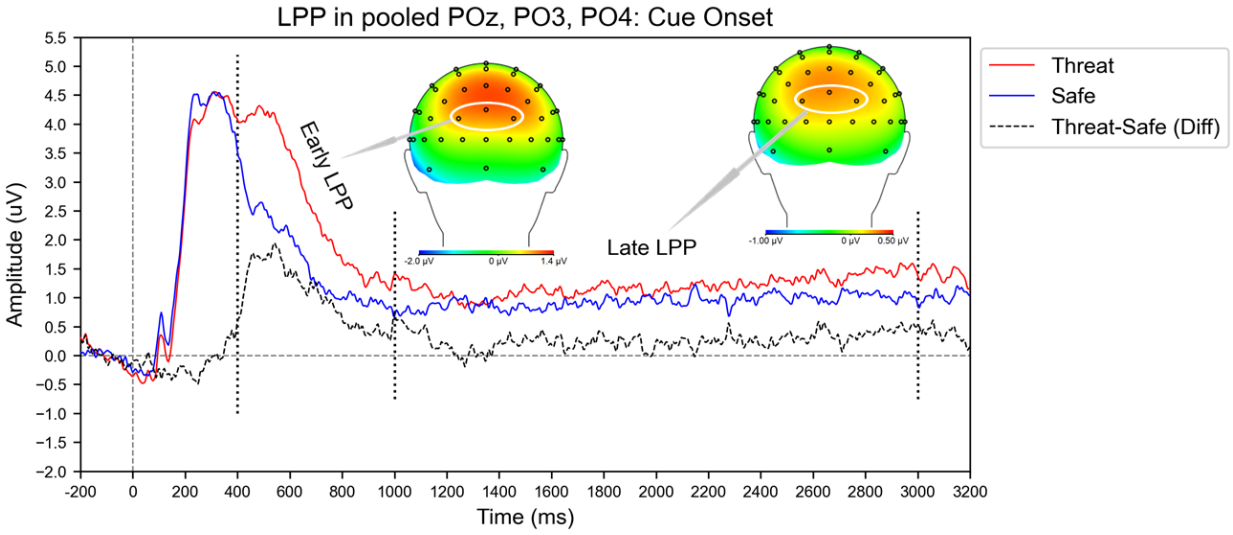

Figure 11. *LPP after cue onset. Early LPP: 400 to 1000ms, Late LPP: 1000 to 3000ms. Topographies display the differences between conditions (Threat - Safe).*

Cue offset: Identification of the electrode and the time window of interest

We also examined LPP after cue offset. Similar to cue onset LPP, we separated the time windows into early (350 to 1000ms) and late (1000 to 3000ms) (Figure 12). For the LPP after cue offset, the highest increase was observed in slightly more anterior regions than after cue onset and therefore the pooled CPz, CP1, CP2 were selected for analysis (Figure 12).

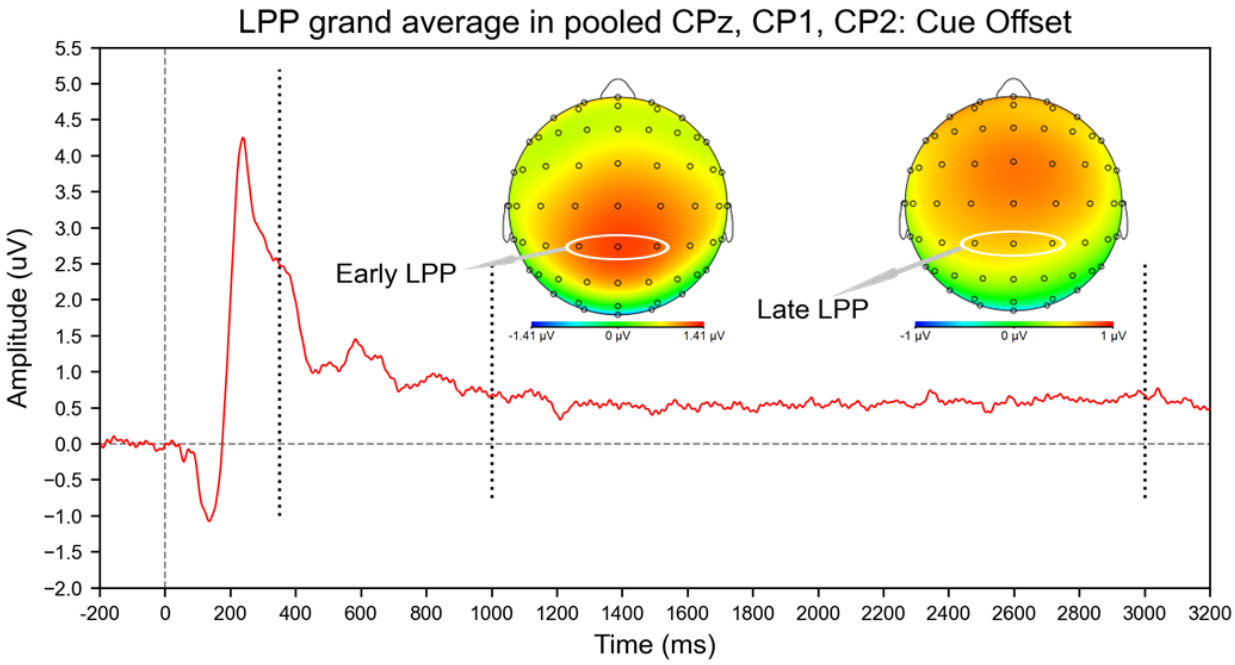

Figure 12. *LPP after cue offset: Grand Average (Pre/post, cTBS, Threat/Safe). Early LPP: 350 to 1000ms, Late LPP: 1000 to 3000ms.*

Cue offset: Statistical analysis

A 3-way RMANOVA for the cue offset LPP data demonstrated a statistically significant main effect of Threat/Safe for both the early LPP ($F_{(1,27)} = 22.888$, $p < 0.001$, Figure 13) and the late LPP ($F_{(1,27)} = 9.083$, $p = 0.006$, Figure 13). In both early and late LPP, we observed a higher amplitude in the threat condition (early: M = 1.449µV, late: M = 0.691µV) than the safe condition (early: M = 0.788µV, late: M = 0.439µV). Moreover, the main effect or interaction of the factor cTBS did not reach statistical significance ($p > 0.1$, Table 3).

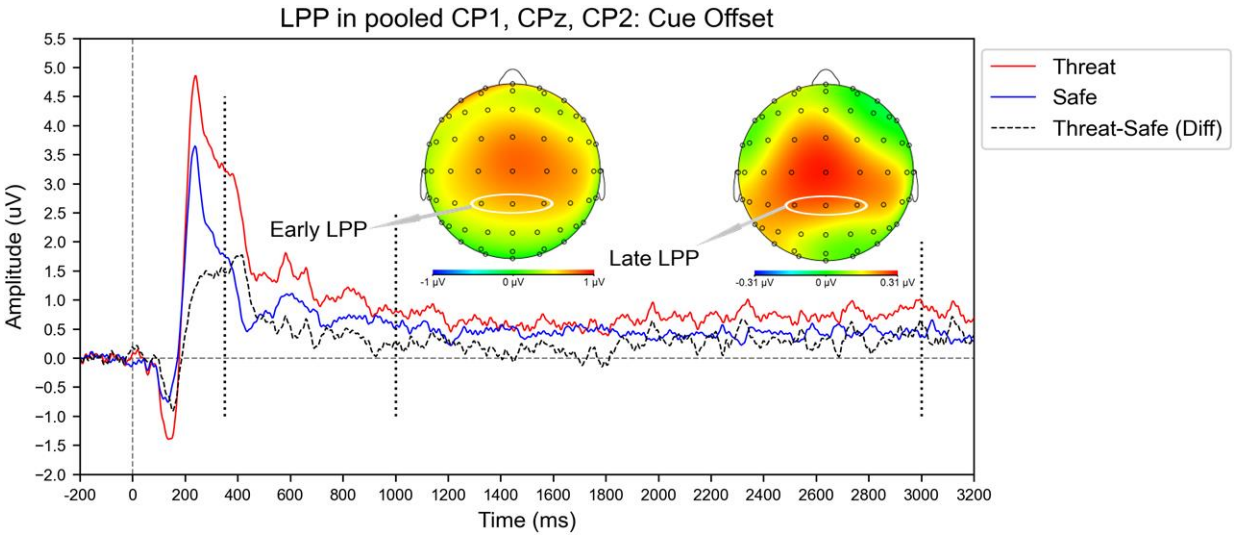

Figure 13. *LPP after cue offset. Early LPP: 350 to 1000ms, Late LPP: 1000 to 3000ms. Topographies display the differences between conditions (Threat - Safe).*

Table 2. *Summary of the brain oscillations results.*

				2x2x2 RMANOVA (cTBS x Pre/Post x Threat/Safe)				2x2 post-cTBS RMANOVA	
				Main effects			Interactions	Main effect	Interaction
		Time window	Electrode site	Threat/Safe	Pre/Post	cTBS	all cTBS interactions	cTBS	cTBS * Threat/Safe
Theta (4 to 8 Hz)	Onset	50 to 450ms	Fronto-Midline (Fz)	1.124	8.410**	F < 1	F < 1	1.15	F < 1
		50 to 450ms	alPFC (pooled AF4 & Fp2)	F < 1	1.931	F < 1	F < 1	2.923	F < 1
	Offset	50 to 450ms	Fronto-Midline (FCz)	16.257****	6.544*	F < 1	F < 1	F < 1	F < 1
		100 to 575ms	alPFC (pooled AF4 & Fp2)	6.547*	2.316	1.717	cTBS * Threat/Safe = 1.346, Rest: F < 1	F < 1	F < 1
Delta (0.5 to 4 Hz)	Onset	50 to 900ms	Fronto-Midline (Fz)	4.463*	5.091*	F < 1	cTBS * Pre/Post = 4.916*, Rest: F < 1	3.787	F < 1
		50 to 900ms	alPFC (pooled AF4 & Fp2)	F < 1	F < 1	1.931	cTBS * Pre/Post = 4.722, cTBS * Threat/Safe = 1.926 Rest: F < 1	6.608*	F < 1
	Offset	100 to 950ms	Fronto-Midline (Fz)	25.244****	1.486	F < 1	cTBS * Pre/Post = 1.072, cTBS * Threat/Safe = 1.570, Rest: F < 1	F < 1	F < 1
		200 to 1200ms	alPFC (pooled AF4 & Fp2)	14.991****	F < 1	F < 1	cTBS * Pre/Post = 1.892, Rest: F < 1	F < 1	F < 1
Alpha (9 to 13 Hz)	Offset	650 to 2150ms	Fronto-Midline (Fz)	5.619*	1.345	1.954	cTBS * Pre/Post * Threat/Safe =1.371, Rest: F < 1	F < 1	F < 1
		650 to 2150ms	Posterior (pooled PO4, PO8, O2)	12.292***	F < 1	F < 1	F < 1	F < 1	F < 1

* p <0.05; ** p < 0.01; *** p < 0.005; **** p < 0.001. $F_{(1,27)}$

Table 3. *Summary of the LPP results.*

			2x2x2 RMANOVA (cTBS x Pre/Post x Threat/Safe)				2x2 post-cTBS RMANOVA	
			Main effects			Interactions	Main effect	Interaction
			Threat/Safe	Pre/Post	cTBS	all cTBS interactions	cTBS	cTBS * Threat/Safe
LPP	Onset (pooled POz, PO3, PO4)	early (400 to 1000ms)	53.735****	F < 1	F < 1	F < 1	F < 1	F < 1
		late (1000 to 3000ms)	13.681****	F < 1	F < 1	cTBS * Pre/Post = 3.093, cTBS * Pre/Post * Threat/Safe = 1.278	F < 1	F < 1
	Offset (pooled CPz, CP1, CP2)	early (350 to 1000ms)	22.888****	1.254	F < 1	cTBS * Threat/Safe = 2.151, Rest: F < 1	F < 1	F = 2.840
		late (1000 to 3000ms)	9.083**	F < 1	F < 1	cTBS * Pre/Post = 1.211, cTBS * Threat/Safe = 1.227, cTBS * Pre/Post * Threat/Safe = 3.308	F < 1	F = 3.903

* p <0.05; ** p < 0.01; *** p < 0.005; **** p < 0.001. $F_{(1,27)}$

Post-hoc analyses: effect of cTBS on the resting state data

To explore the non-task related effects of cTBS on resting state EEG data, we explored changes in the power density ($\mu V^2/Hz$) of delta (0.5 to 4 Hz), theta (4 to 8 Hz), alpha (8 to 12 Hz), and beta (12 to 30 Hz) during the startle habituation period. Although still nonsignificant, the largest difference between active and control cTBS was observed in the delta range (paired-samples t-test: t(27) = -1.607, p = 0.120, Figure 14). Paired samples t-tests for other frequencies (theta, alpha, beta) revealed no significant difference between the active and control stimulation.

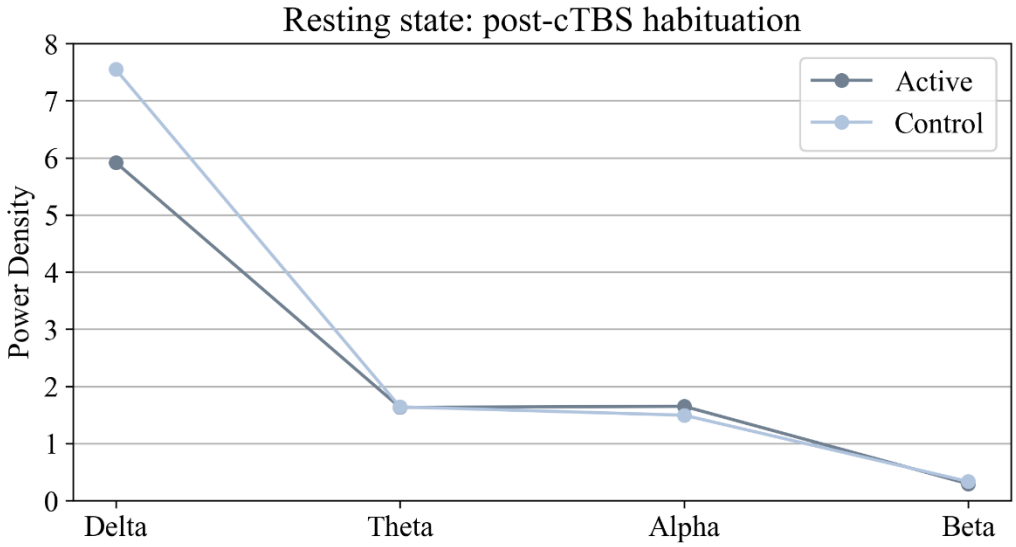

Figure 14. *Effect of cTBS on different frequency bands during the habituation phase*

Therefore, we further explored the development of the impact of cTBS on delta oscillations throughout the task. In addition to the startle habitation period, we also examined the cue offset period in the instructed fear task, during which participants are instructed to rest. For this analysis, the task data was separated into four parts and the delta power densities were exported from each quarter. We conducted a 2-way RMANOVA with a 5-level factor 'Time' (Habituation, Quarter 1, Quarter 2, Quarter 3, Quarter 4) and 'cTBS' (Active/Control). However, the effect of cTBS on delta oscillations was not stable throughout the task (Figure 15) and the 2-way RMANOVA showed a non-significant main effect of cTBS ($F_{(1,27)} = 0.387$, p

= 0.539). The biggest difference between the active and control conditions seems to be present during the habituation period and the first quarter of the task (Figure 15). However, a subsequent 2x2 RMANOVA (factors: 'Time' = Habituation, Quarter 1 and 'cTBS' = Active/Control) showed that this difference still remained non-significant ($F_{(1,27)} = 2.904$, $p = 0.100$).

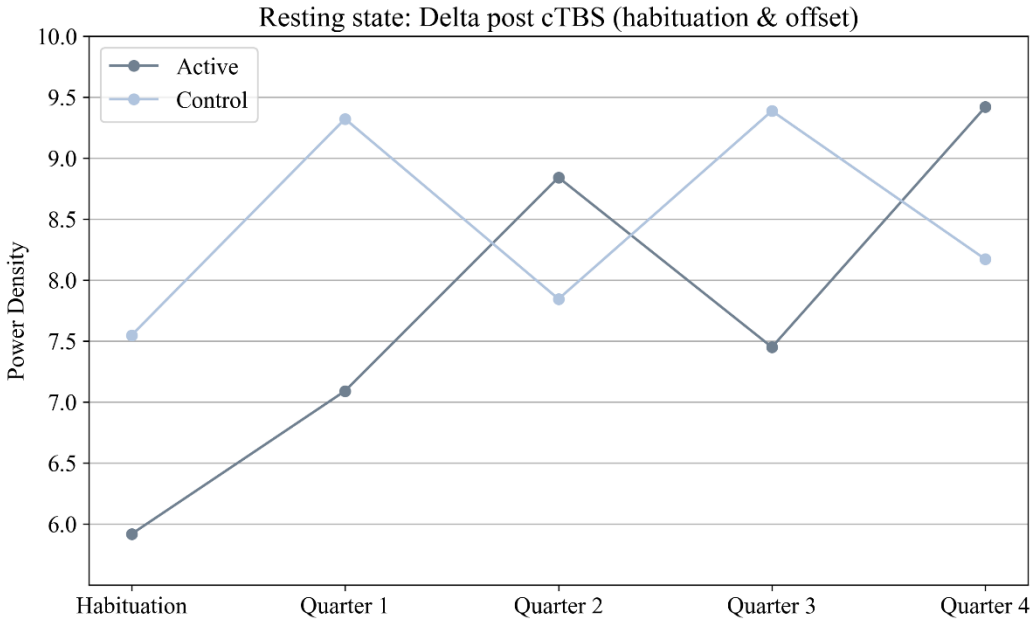

Figure 15. *Effect of cTBS on delta oscillations during the habituation phase and the offset periods during the task*

Discussion

The aim of this study was to replicate previous findings by van Dijk et al. (2017) and to extend them by measuring EEG. This thesis focuses on the EEG part of this project. We examined what oscillatory bands are involved in the instructed fear task. Furthermore, we investigated the impact of cTBS over the alPFC on brain oscillations and LPP. The alPFC has been found to be involved in fear downregulation (Klumpers et al., 2010; van Dijk et al., 2017) and emotion regulation (Bramson et al., 2018; 2020). Theta oscillations localized to alPFC have been reported to play a role in regulating emotional behavior (Bramson et al., 2018). Another study reported increased theta power during cognitive reappraisal (Ertl et al., 2013). These

studies have led us to hypothesize a possible involvement of alPFC-theta oscillations in fear downregulation. Furthermore, based on the previous research, we hypothesized that fronto-medial theta, which is likely generated in the dmPFC, would be the main oscillatory band involved in fear expression (Mueller et al., 2014; Sperl et al., 2019). Moreover, we hypothesized that active cTBS over alPFC would lead to a decreased fear regulation and hence increased fear expression. Our results indicate that cTBS did not influence theta oscillations or LPP. Moreover, contrary to the expected increase of theta power during the presentation of the threat versus safe cue caused by stronger fear expression, our results showed a non-significant difference between the cue conditions after cue onset. Instead of differences in theta, we found higher delta power during the threat cue than the safe cue, indicating a possible involvement of delta oscillations in fear processing. After cue offset, we observed higher theta power for threat versus safe stimuli. It remains unclear whether this increase reflects an ongoing fear expression elicited by the cue or if it reflects the fear downregulation process. Similarly, after cue offset, higher power in the threat versus safe condition was also observed in delta and alpha oscillations. Successful threat manipulation was confirmed by increased LPP in the threat condition after both cue onset and offset.

Previous studies have reported that theta oscillations are involved in fear expression. The scalp topographies in these studies show the highest theta increase in fronto-midline areas, which was source localized to the dmPFC area by using a low-resolution brain electromagnetic tomography (LORETA) (Mueller et al., 2014; Sperl et al., 2019). It was outside of the scope of this thesis to apply LORETA (Pascual-Marqui et al., 2002) to identify the source of theta. In line with these studies, the scalp topographies for the cue onset data (Figure 3B) showed a similar fronto-medial theta increase with a possible source in the dmPFC. Moreover, the observed fronto-medial theta increase also encompassed electrodes that correspond with the cortical location of alPFC, which is consistent with van Dijk et al. (2017) who found that the

alPFC contributes to fear downregulation not only after threat offset, but also during the presentation of the cue.

Contrary to our hypothesis, we did not find a difference in theta power between the threat and safe condition after cue onset. The initial cue onset analyses focused on the Fz electrode (as in Mueller et al., 2014; Sperl et al., 2019) and pooled AF4 & Fp2 electrodes that correspond with the anatomical location of alPFC (Bramson et al., 2018). We also conducted additional post-hoc analyses on an array of 15 electrodes (from Pre-Frontal (Fp) to Central (Cz) electrodes). These analyses revealed that theta power during cue presentation did not differ between threat and safe condition in any subset of these electrodes (Appendix 1). Because the highest theta increase occurred during an early time window of 50 to 450ms (Figure 3A), our analyses focused on this time bin. Although the lack of difference between conditions after cue onset was unexpected, it is possible that the difference between threat and safe condition occurred later during the cue processing and this initial theta power increase reflects a different function of theta oscillations, such as signaling for cognitive control (Cavanagh & Cohen, 2022), which occurred to the same extent for both threat and safe condition. Even though the theta increase in response to the cue onset encompassed the whole theta range (4 to 8 Hz, Figure 2), there is a chance that the difference between threat versus safe conditions occurs only at a specific frequency (e.g., 6 Hz as in Bramson et al. 2018) and therefore, a more fine-grained analysis focusing on specific frequencies would be necessary to uncover these differences. Although all of these potential explanations for the lack of difference between conditions in theta power during the cue presentation are valid, it still remains unclear why our study did not find theta oscillations to be stronger in the threat versus safe condition given that the involvement of theta in fear expression seems to be a well-established finding (Chen et al., 2021; Sperl et al., 2019; Mueller et al., 2014; DeLaRosa et al., 2014; Chirumamilla et al., 2019).

Instead of the hypothesized theta power differences between cue onset conditions, we observed this difference in the delta range. Delta oscillations have been found to be associated with basic biological motivations, detecting motivationally salient stimuli, with attention (Knyazev, 2012), and importantly, also emotion processing. It has been suggested that delta oscillations could serve as a marker of emotional processing (Klados et al., 2009). Therefore, our results are in line with this study, as it is expected that the threat stimulus elicits more intense emotional processing than the safe stimulus. Our results also suggest that the more intense emotional processing during the threat stimulus persists even after the cue offset, as reflected in a higher delta power in the threat condition than the safe condition after cue offset.

As hypothesized, after cue offset, there was a higher power of theta in the threat condition compared to the safe condition. Previous studies have shown that the downregulation of fear after threat offset is a rapid process (Klumpers et al., 2010; van Dijk et al., 2017). The increase in theta oscillations after cue offset occurred during the same period as the suspected process of fear downregulation. Therefore, due to the temporal characteristics of the theta increase after cue offset and the evidence that theta oscillations are involved in emotion regulation (Bramson et al., 2018; Ertl et al., 2013), it may seem that the increase in theta power at threat offset could reflect the process of fear downregulation.

A previous study reported that the source of theta that mediates regulation of emotional behavior is alPFC (Bramson et al., 2018). However, the topography of our grand averaged data across all participants and conditions shows that the highest increase occurred in the fronto-central areas. The power increase in electrodes that would be consistent with a source in alPFC was weaker, occurred later in time, and was slightly longer than in the fronto-central electrode (Figure 4A). However, the topography of the conditions difference shows that the anterior/frontal electrodes capture the difference between the cue conditions most sensitively (Figure 4G). Furthermore, the condition differences have a similar temporal dynamic as the

grand averaged data with alPFC theta power difference peaking later and being more prolonged than the fronto-medial theta (Figure 4D). Based on the topographical and temporal dynamics, it is theoretically possible that the fronto-medial theta increase might reflect the ongoing process of fear expression. However, the slightly later occurrence of the theta increase in electrodes consistent with the alPFC location might reflect the simultaneously occurring process of fear downregulation. However, until a more fine-grained analysis focusing on shorter time windows that would potentially separate the earlier process of fear expression and the later process of fear downregulation is done, these interpretations are a theoretical possibility and should be interpreted with caution.

In addition to theta and alpha oscillations, higher power in the threat versus safe cue was also found in the alpha band. It has been suggested that alpha oscillations might mediate the inhibition of task-irrelevant cortical regions, which in turn causes an increase of internally as opposed to externally focused attention (Klimesch et al., 2007). A recent study found higher alpha power after threat offset in a group that received anxiolytic placebo treatment compared to a group that did not receive any treatment. They propose that as a result of the placebo manipulation, this group might have been focusing their attention more internally, which resulted in a better downregulation of sustained anxiety as reflected by increased alpha. They argue that alpha oscillations directly contributed to the placebo effect (Meyer et al., 2015). Our data is in line with the above-mentioned studies because the increased alpha power at threat offset might reflect increased inhibition of the task-irrelevant areas and a stronger internally focused attention evoked by the preceding threat stimulus.

We found no effect of cTBS on theta oscillations or LPP during the instructed fear task. The reason for the lack of effect of cTBS on theta power or LPP is unclear. The only oscillatory band in which an effect of cTBS was found was in the delta range after cue onset. After active cTBS, there was a general decrease of delta power across the threat and safe cues. Taken into

account that alPFC has been found to play a general role in fear downregulation (van Dijk et al., 2017) and delta oscillations are involved in emotional processing (Klados et al., 2009), one would rather expect to find an increase in delta power after active cTBS due to the decreased ability of alPFC to downregulate fear, resulting in a heightened emotional processing. Therefore, the reason for the general decrease of delta power after active cTBS remains unclear.

We conducted further exploratory analyses on the impact of cTBS on the resting state EEG brain oscillations. Similar to the instructed fear task, the only oscillatory band that showed some impact of cTBS during resting state was delta. This effect was not statistically significant and therefore, it must be interpreted with caution. After active cTBS, delta power density slightly decreased. However, this effect was weak and short-lived and by the second quarter of the task it was no longer present. We are unable to exclude the possibility that the cTBS did not have an influence on the brain or that the impact of cTBS was not captured by brain oscillations.

We found increased LPP in the threat versus safe condition both after cue onset and cue offset. The threat cue signals the possibility of an upcoming electric shock. Therefore, our findings are in line with the theory that LPP is modulated by the stimulus significance (Hajcak & Foti, 2020), as it is expected that a threatening stimulus has a higher stimulus significance than the safe stimulus. Furthermore, the increased stimulus significance of the threat versus safe cue persists even after the cue offset, as reflected by a higher LPP amplitude. LPP has also been referred to as a feasible marker of fear processing (Gonzalez-Escamilla et al., 2018) and therefore, these findings confirm successful threat manipulation.

Our current study is a replication of a study conducted by van Dijk et al. (2017), with the extension of EEG. Same as in van Dijk et al. (2017), our study also measured startle response, skin conductance, and subjective ratings. The results of these measures are reported by Rodenburg et al. (2022). Van Dijk et al. (2017), reported a significant increase in startle magnitude after cTBS over alPFC, especially in the threat condition, indicating a role of the

alPFC in fear downregulation. Although the startle results in our study were not entirely consistent, Rodenburg et al. (2022) concludes that we failed to replicate the previous findings by van Dijk et al. (2017). Similar findings were obtained for skin conductance and subjective fear ratings. Therefore, the EEG results are in line with the other measurements, and it is possible that the cTBS did not influence the brain in the hypothesized manner.

Limitations and future directions

One of the limitations of our study is the lack of neuronavigation when applying cTBS. Some studies adjust the stimulation site based on the Montreal Neurological Institute (MNI) coordinates obtained by MRI, which ensures a successful targeting of a particular brain region (Okamoto et al., 2004). However, because we only used the EEG cap to standardize the stimulation site, it is possible that individual anatomical differences resulted in incorrect cTBS targeting of the alPFC and vertex. Furthermore, given the evidence that cTBS might influence the activity in the interconnected regions of the target site (Bestmann & Feredoes, 2013), we cannot fully exclude the possibility that the cTBS had an impact in different brain regions.

In addition to analyzing the oscillatory mechanisms during the instructed fear task, we also conducted exploratory analysis of resting state data. However, it must be noted that we did not record clean resting state data. As a substitute, we used the startle habituation period at the beginning of the task and the intertrial intervals during the task. Although we excluded the periods around the startle probe for the habituation period and we only used the intertrial intervals after the time required for fear downregulation in the instructed fear task (van Dijk et al., 2017), our resting state data differs from the traditionally collected resting states, which are a continuous EEG measure of an instructed rest. Therefore, it would be useful for future cTBS-EEG studies to include a standard EEG resting state measure.

The research of the impact of cTBS on brain oscillations is scarce and it would be highly beneficial for future studies to determine which EEG resting state markers are influenced by the cTBS. In addition to oscillatory power and regional synchronization that have been found to be influenced by cTBS (Noh et al., 2012), another possible marker that could capture the impact of cTBS on brain oscillations is prefrontal brain asymmetry. Alpha asymmetry has been found to be a marker of a risk for depression (Stewart et al., 2010), as well as an indicator of emotion-related personality traits (Allen et al., 2018). Since the excitability of a particular brain region decreases after cTBS, this decrease could be potentially captured by a shift in the alpha asymmetry after active cTBS from one brain hemisphere to the other, especially when targeting brain regions involved in emotional processing. Another potential marker to explore could be the theta/beta ratio. It has been found that increased theta/beta ratio might represent a reduction in the prefrontal cortical control of the subcortical affective drive (Putman et al., 2010). Low theta/beta ratio is linked with better cognitive control of emotional processing as opposed to high theta/beta ratio (Angelidis et al., 2018). A cTBS-induced inhibition of regions involved in cognitive control might result in a shift in the theta/beta ratio. After active cTBS over a brain region involved in cognitive control, it could be expected to observe an increase in the theta/beta ratio caused by decreased cognitive control abilities. Establishing a framework of EEG markers that are expected to be influenced by cTBS would be useful for confirming the effectiveness of the impact of cTBS on EEG mechanisms in general.

Regardless of cTBS, our hypotheses operate with the possibility of different sources and different functions of theta oscillations taking place after cue offset in the instructed fear task. However, EEG is known for its high temporal, but low spatial resolution. Therefore, in addition to the above-mentioned suggestions for future work with this dataset, applying the current source density (CSD) methodology could be useful for improving the spatial resolution of the EEG signal (Kayser & Tenke, 2015). Moreover, to determine the source of theta oscillations

after cue offset, it might be beneficial to apply LORETA (Pascual-Marqui, 2002). By determining to source of theta either to dmPFC or alPFC, we could make stronger interpretations of the function of theta increase observed after threat versus safe cue offset by using the current evidence of the processes that these regions are involved in.

There is a substantial amount of evidence for the involvement of vmPFC in fear extinction (Milad & Quirk, 2012) and fear downregulation (Klumpers et al., 2010). However, the research of vmPFC-elicited brain oscillations involved in these processes is limited. There is some evidence that shows that vmPFC-localized gamma oscillations might be involved in the recall of fear extinguished stimuli (Mueller et al., 2014). However, these findings were unconfirmed by a follow-up study (Bierwirth et al., 2021). For the future work with this dataset, it might be beneficial to explore the potential involvement of gamma oscillation in fear downregulation after cue offset. One of the possible reasons for the lack of research on the vmPFC oscillatory mechanisms involved in fear extinction and fear downregulation might be that its ventromedial position makes it difficult to reliably record EEG signal with scalp EEG. One of the potential ways to overcome this problem would be by using nasopharyngeal electrodes that might be able to record vmPFC activity better than scalp EEG. It would be beneficial for future studies to explore the oscillatory mechanisms elicited by vmPFC involved in fear extinction and fear downregulation.

For future directions, it might be valuable to explore the relationship between LPP and theta & delta oscillations. Originally, it has been proposed that delta and theta bands are the main features of LPP (Başar et al., 1984); however, more recent evidence specifies that LPP might reflect a phase resetting of delta oscillations elicited by emotionally arousing stimuli (Schroeder & Lakatos, 2009). It has been suggested that LPP represents a global inhibition of the visual cortex, which causes the survival of selective activity involved in emotion processing (Brown et al., 2012). In line with this notion, the visual system of the brain has been identified

as the generator of LPP (Sabatinelli et al., 2007). In addition to the visual system, an fMRI-EEG study reported that LPP was also coupled with a broad brain network consisting of cortical and subcortical structures that are involved in emotional processing. Furthermore, they reported that the LPP elicited by positive stimuli is coupled with different brain regions than the LPP elicited by negative stimuli. For the negative stimuli, LPP was coupled with the activation of the ventrolateral PFC, insula, and posterior cingulate cortex (Liu et al., 2012). Neither the typical centroparietal topography, nor the described LPP sources (Liu et al., 2012) overlap with the fronto-medial theta oscillation involved in fear expression (Mueller et al., 2014; Sperl et al., 2019). Therefore, even though LPP and theta oscillations might be, in some cases, evoked by similar experimental conditions (e.g., fear expression), they probably reflect different processes. It might be feasible that theta oscillations are involved in the activation of the fear response, whereas LPP might reflect the downstream consequences of emotional processing (J. Baas, personal communication, November 7, 2022) evoked by the subcortical brain areas, such as the amygdala (Liu et al., 2012). Furthermore, because it was postulated that LPP might reflect phase resetting of delta oscillations (Schroeder & Lakatos, 2009), and the evidence of the involvement of delta oscillations in emotional processing (Klados et al., 2009), it is likely that there is a closer functional overlap between LPP and delta oscillations rather than theta oscillations. More research is needed to identify the oscillatory features of LPP and to explore their relationship, the similarities in their functional overlap and the source of generation.

Conclusion

To conclude, the cTBS over the alPFC did not impact theta oscillations or LPP during fear expression or fear downregulation. It remains unclear whether the lack of effect of cTBS over alPFC on theta oscillations is caused by an insufficient involvement of alPFC in fear downregulation, or the cTBS over alPFC did not sufficiently influence theta oscillations, or because the cTBS did not have an impact on the brain. Moreover, contrary to our hypothesis,

we did not find theta oscillations to play a role in fear expression during the cue presentation. Instead of theta, we found that oscillations in the delta range were stronger in the threat versus safe cue. In line with previous research, our study adds more evidence for the involvement of delta oscillations in emotional processing (Klados et al., 2009). At the cue offset, we found an increase in theta power in the threat versus safe condition. However, it remains unclear whether the theta increase in threat versus safe condition after cue offset reflects the ongoing fear expression elicited by the threat cue or the process of fear downregulation. Furthermore, there was also an increase in delta and alpha oscillations after cue offset. Increased delta at threat offset might indicate an ongoing increased emotional processing, whereas increased alpha might represent increased inhibition of task-irrelevant areas, resulting in a higher internally focused attention (Meyer et al., 2015).

Bibliography:

Allen, J. J. B., Keune, P. M., Schönenberg, M., & Nusslock, R. (2018). Frontal EEG alpha asymmetry and emotion: From neural underpinnings and methodological considerations to psychopathology and social cognition. *Psychophysiology*, *55*(1). https://doi.org/10.1111/psyp.13028

Angelidis, A., Hagenaars, M., van Son, D., van der Does, W., & Putman, P. (2018). Do not look away! Spontaneous frontal EEG theta/beta ratio as a marker for cognitive control over attention to mild and high threat. *Biological Psychology*, *135*, 8–17. https://doi.org/10.1016/j.biopsycho.2018.03.002

Bacigalupo, F., & Luck, S. J. (2018). Event-related potential components as measures of aversive conditioning in humans. *Psychophysiology*, *55*(4), e13015. https://doi.org/10.1111/psyp.13015

Barbas, H. (2000). Connections underlying the synthesis of cognition, memory, and emotion in primate prefrontal cortices. *Brain Research Bulletin*, *52*(5), 319–330. https://doi.org/10.1016/S0361-9230(99)00245-2

Başar, E., Başar-Eroglu, C., Rosen, B., & Schütt, A. (1984). A New Approach to Endogenous Event-Related Potentials in Man: Relation Between Eeg and P300-Wave. *International Journal of Neuroscience*, *24*(1), 1–21. https://doi.org/10.3109/00207458409079530

Bestmann, S., & Feredoes, E. (2013). Combined neurostimulation and neuroimaging in cognitive neuroscience: Past, present, and future. *Annals of the New York Academy of Sciences*, *1296*(1), 11–30. https://doi.org/10.1111/nyas.12110

Bierwirth, P., Sperl, M. F. J., Antov, M. I., & Stockhorst, U. (2021). Prefrontal Theta Oscillations Are Modulated by Estradiol Status During Fear Recall and Extinction Recall. *Biological Psychiatry: Cognitive Neuroscience and Neuroimaging*, *6*(11), 1071–1080. https://doi.org/10.1016/j.bpsc.2021.02.011

BrainVision Analyzer (Version 2.1) [Software]. (2017). Gilching, Germany: Brain Products GmbH.

Bramson, B., Folloni, D., Verhagen, L., Hartogsveld, B., Mars, R. B., Toni, I., & Roelofs, K. (2020). Human Lateral Frontal Pole Contributes to Control over Emotional Approach–Avoidance Actions. *Journal of Neuroscience*, *40*(14), 2925–2934. https://doi.org/10.1523/JNEUROSCI.2048-19.2020

Bramson, B., Jensen, O., Toni, I., & Roelofs, K. (2018). Cortical Oscillatory Mechanisms Supporting the Control of Human Social–Emotional Actions. *Journal of Neuroscience*, *38*(25), 5739–5749. https://doi.org/10.1523/JNEUROSCI.3382-17.2018

Brown, S., van Steenbergen, H., Band, G., de Rover, M., & Nieuwenhuis, S. (2012). Functional significance of the emotion-related late positive potential. *Frontiers in Human Neuroscience*, *6*. https://www.frontiersin.org/articles/10.3389/fnhum.2012.00033

Cavanagh, J. F., Eisenberg, I., Guitart-Masip, M., Huys, Q., & Frank, M. J. (2013). Frontal Theta Overrides Pavlovian Learning Biases. *Journal of Neuroscience*, *33*(19), 8541–8548. https://doi.org/10.1523/JNEUROSCI.5754-12.2013

Cavanagh, J. F., & Shackman, A. J. (2015). Frontal midline theta reflects anxiety and cognitive control: Meta-analytic evidence. *Journal of Physiology-Paris*, *109*(1), 3–15. https://doi.org/10.1016/j.jphysparis.2014.04.003

Chen, S., Tan, Z., Xia, W., Gomes, C. A., Zhang, X., Zhou, W., Liang, S., Axmacher, N., & Wang, L. (2021). Theta oscillations synchronize human medial prefrontal cortex and amygdala during fear learning. *Science Advances*, *7*(34), eabf4198. https://doi.org/10.1126/sciadv.abf4198

Chien, J. H., Colloca, L., Korzeniewska, A., Cheng, J. J., Campbell, C. M., Hillis, A. E., & Lenz, F. A. (2017). Oscillatory EEG activity induced by conditioning stimuli during fear conditioning

reflects Salience and Valence of these stimuli more than Expectancy. *Neuroscience*, *346*, 81–93. https://doi.org/10.1016/j.neuroscience.2016.12.047

Chirumamilla, V. C., Gonzalez-Escamilla, G., Koirala, N., Bonertz, T., von Grotthus, S., Muthuraman, M., & Groppa, S. (2019). Cortical Excitability Dynamics During Fear Processing. *Frontiers in Neuroscience*, *13*. https://www.frontiersin.org/articles/10.3389/fnins.2019.00568

Cohen, M. X. (2014). *Analyzing Neural Time Series Data: Theory and Practice*. MIT Press.

DeLaRosa, B. L., Spence, J. S., Shakal, S. K. M., Motes, M. A., Calley, C. S., Calley, V. I., Hart, J., & Kraut, M. A. (2014). Electrophysiological spatiotemporal dynamics during implicit visual threat processing. *Brain and Cognition*, *91*, 54–61. https://doi.org/10.1016/j.bandc.2014.08.003

Ertl, M., Hildebrandt, M., Ourina, K., Leicht, G., & Mulert, C. (2013). Emotion regulation by cognitive reappraisal—The role of frontal theta oscillations. *NeuroImage*, *81*, 412–421. https://doi.org/10.1016/j.neuroimage.2013.05.044

Etkin, A., & Wager, T. D. (2007). Functional Neuroimaging of Anxiety: A Meta-Analysis of Emotional Processing in PTSD, Social Anxiety Disorder, and Specific Phobia. *American Journal of Psychiatry*, *164*(10), 1476–1488. https://doi.org/10.1176/appi.ajp.2007.07030504

Field, A. (2013). *Discovering Statistics Using IBM SPSS Statistics*. SAGE.

Folloni, D., Sallet, J., Khrapitchev, A. A., Sibson, N., Verhagen, L., & Mars, R. B. (2019). Dichotomous organization of amygdala/temporal-prefrontal bundles in both humans and monkeys. *ELife*, *8*, e47175. https://doi.org/10.7554/eLife.47175

Fullana, M. A., Albajes-Eizagirre, A., Soriano-Mas, C., Vervliet, B., Cardoner, N., Benet, O., Radua, J., & Harrison, B. J. (2018). Fear extinction in the human brain: A meta-analysis of fMRI studies in healthy participants. *Neuroscience & Biobehavioral Reviews*, *88*, 16–25. https://doi.org/10.1016/j.neubiorev.2018.03.002

Cavanagh, J. M., Cohen, M. X. (2022). Frontal midline theta as a model specimen of cortical theta in Gable, P., Miller, M., & Bernat, E. (Eds.), *The Oxford Handbook of EEG Frequency* (pp. 178-201). Oxford University Press.

Ghashghaei, H. T., & Barbas, H. (2002). Pathways for emotion: Interactions of prefrontal and anterior temporal pathways in the amygdala of the rhesus monkey. *Neuroscience*, *115*(4), 1261–1279. https://doi.org/10.1016/S0306-4522(02)00446-3

Gonzalez-Escamilla, G., Chirumamilla, V. C., Meyer, B., Bonertz, T., von Grotthus, S., Vogt, J., Stroh, A., Horstmann, J.-P., Tüscher, O., Kalisch, R., Muthuraman, M., & Groppa, S. (2018). Excitability regulation in the dorsomedial prefrontal cortex during sustained instructed fear responses: A TMS-EEG study. *Scientific Reports*, *8*(1), Article 1. https://doi.org/10.1038/s41598-018-32781-9

Gratton, G., Coles, M. G. H., & Donchin, E. (1983). A new method for off-line removal of ocular artifact. *Electroencephalography and Clinical Neurophysiology*, *55*(4), 468–484. https://doi.org/10.1016/0013-4694(83)90135-9

Grillon, C., & Ameli, R. (1998). Effects of threat of shock, shock electrode placement and darkness on startle. *International Journal of Psychophysiology*, *28*(3), 223–231. https://doi.org/10.1016/S0167-8760(97)00072-X

Grillon, C., & Baas, J. (2003). A review of the modulation of the startle reflex by affective states and its application in psychiatry. *Clinical Neurophysiology*, *114*(9), 1557–1579. https://doi.org/10.1016/S1388-2457(03)00202-5

Groenewegen, H. J., Wright, C. I., & Uylings, H. B. M. (1997). The anatomical relationships of the prefrontal cortex with limbic structures and the basal ganglia. *Journal of Psychopharmacology*, *11*(2), 99–106. https://doi.org/10.1177/026988119701100202

Hajcak, G., & Foti, D. (2020). Significance?... Significance! Empirical, methodological, and theoretical connections between the late positive potential and P300 as neural responses to stimulus significance: An integrative review. *Psychophysiology*, *57*(7), e13570. https://doi.org/10.1111/psyp.13570

Hajcak, G., & Nieuwenhuis, S. (2006). Reappraisal modulates the electrocortical response to unpleasant pictures. *Cognitive, Affective, & Behavioral Neuroscience*, *6*(4), 291–297. https://doi.org/10.3758/CABN.6.4.291

Hajcak, G., & Olvet, D. M. (2008). The persistence of attention to emotion: Brain potentials during and after picture presentation. *Emotion*, *8*, 250–255. https://doi.org/10.1037/1528-3542.8.2.250

IBM Corp. Released 2021. IBM SPSS Statistics for Windows, Version 28.0. Armonk, NY: IBM Corp

Kamali, A., Sair, H. I., Blitz, A. M., Riascos, R. F., Mirbagheri, S., Keser, Z., & Hasan, K. M. (2016). Revealing the ventral amygdalofugal pathway of the human limbic system using high spatial resolution diffusion tensor tractography. *Brain Structure and Function*, *221*(7), 3561–3569. https://doi.org/10.1007/s00429-015-1119-3

Karalis, N., Dejean, C., Chaudun, F., Khoder, S., Rozeske, R. R., Wurtz, H., Bagur, S., Benchenane, K., Sirota, A., Courtin, J., & Herry, C. (2016). 4-Hz oscillations synchronize prefrontal–amygdala circuits during fear behavior. *Nature Neuroscience*, *19*(4), Article 4. https://doi.org/10.1038/nn.4251

Kayser, J., & Tenke, C. E. (2015). On the benefits of using surface Laplacian (Current Source Density) methodology in electrophysiology. *International Journal of Psychophysiology : Official Journal of the International Organization of Psychophysiology*, *97*(3), 171–173. https://doi.org/10.1016/j.ijpsycho.2015.06.001

Keel, J. C., Smith, M. J., & Wassermann, E. M. (2001). A safety screening questionnaire for transcranial magnetic stimulation. *Clinical Neurophysiology: Official Journal of the International Federation of Clinical Neurophysiology*, *112*(4), 720. https://doi.org/10.1016/s1388-2457(00)00518-6

Klados, M. A., Frantzidis, C., Vivas, A. B., Papadelis, C., Lithari, C., Pappas, C., & Bamidis, P. D. (2009). A Framework Combining Delta Event-Related Oscillations (EROs) and Synchronisation Effects (ERD/ERS) to Study Emotional Processing. *Computational Intelligence and Neuroscience*, *2009*, e549419. https://doi.org/10.1155/2009/549419

Klimesch, W., Sauseng, P., & Hanslmayr, S. (2007). EEG alpha oscillations: The inhibition–timing hypothesis. *Brain Research Reviews*, *53*(1), 63–88. https://doi.org/10.1016/j.brainresrev.2006.06.003

Klumpers, F., Heitland, I., Oosting, R. S., Kenemans, J. L., & Baas, J. M. P. (2012). Genetic variation in serotonin transporter function affects human fear expression indexed by fear-potentiated startle. *Biological Psychology*, *89*(2), 277–282. https://doi.org/10.1016/j.biopsycho.2011.10.018

Klumpers, F., Raemaekers, M. A. H. L., Ruigrok, A. N. V., Hermans, E. J., Kenemans, J. L., & Baas, J. M. P. (2010). Prefrontal Mechanisms of Fear Reduction After Threat Offset. *Biological Psychiatry*, *68*(11), 1031–1038. https://doi.org/10.1016/j.biopsych.2010.09.006

Knyazev, G. G. (2012). EEG delta oscillations as a correlate of basic homeostatic and motivational processes. *Neuroscience & Biobehavioral Reviews*, *36*(1), 677–695. https://doi.org/10.1016/j.neubiorev.2011.10.002

Lefaucheur, J.-P., Aleman, A., Baeken, C., Benninger, D. H., Brunelin, J., Di Lazzaro, V., Filipović, S. R., Grefkes, C., Hasan, A., Hummel, F. C., Jääskeläinen, S. K., Langguth, B., Leocani, L., Londero, A., Nardone, R., Nguyen, J.-P., Nyffeler, T., Oliveira-Maia, A. J., Oliviero, A., …

Ziemann, U. (2020). Evidence-based guidelines on the therapeutic use of repetitive transcranial magnetic stimulation (rTMS): An update (2014–2018). *Clinical Neurophysiology*, *131*(2), 474–528. https://doi.org/10.1016/j.clinph.2019.11.002

Liu, Y., Huang, H., McGinnis-Deweese, M., Keil, A., & Ding, M. (2012). Neural Substrate of the Late Positive Potential in Emotional Processing. *Journal of Neuroscience*, *32*(42), 14563–14572. https://doi.org/10.1523/JNEUROSCI.3109-12.2012

MacNamara, A., Jackson, T. B., Fitzgerald, J. M., Hajcak, G., & Phan, K. L. (2019). Working Memory Load and Negative Picture Processing: Neural and Behavioral Associations With Panic, Social Anxiety, and Positive Affect. *Biological Psychiatry: Cognitive Neuroscience and Neuroimaging*, *4*(2), 151–159. https://doi.org/10.1016/j.bpsc.2018.04.005

MacNamara, A., Joyner, K., & Klawohn, J. (2022). Event-related potential studies of emotion regulation: A review of recent progress and future directions. *International Journal of Psychophysiology*, *176*, 73–88. https://doi.org/10.1016/j.ijpsycho.2022.03.008

Méndez-Bértolo, C., Moratti, S., Toledano, R., Lopez-Sosa, F., Martínez-Alvarez, R., Mah, Y. H., Vuilleumier, P., Gil-Nagel, A., & Strange, B. A. (2016). A fast pathway for fear in human amygdala. *Nature Neuroscience*, *19*(8), Article 8. https://doi.org/10.1038/nn.4324

Meyer, B., Yuen, K. S. L., Ertl, M., Polomac, N., Mulert, C., Büchel, C., & Kalisch, R. (2015). Neural Mechanisms of Placebo Anxiolysis. *Journal of Neuroscience*, *35*(19), 7365–7373. https://doi.org/10.1523/JNEUROSCI.4793-14.2015

Milad, M. R., Quinn, B. T., Pitman, R. K., Orr, S. P., Fischl, B., & Rauch, S. L. (2005). Thickness of ventromedial prefrontal cortex in humans is correlated with extinction memory. *Proceedings of the National Academy of Sciences of the United States of America*, *102*(30), 10706–10711. https://doi.org/10.1073/pnas.0502441102

Milad, M. R., & Quirk, G. J. (2012). Fear Extinction as a Model for Translational Neuroscience: Ten Years of Progress. *Annual Review of Psychology*, *63*, 129–151. https://doi.org/10.1146/annurev.psych.121208.131631

Milad, M. R., Wright, C. I., Orr, S. P., Pitman, R. K., Quirk, G. J., & Rauch, S. L. (2007). Recall of Fear Extinction in Humans Activates the Ventromedial Prefrontal Cortex and Hippocampus in Concert. *Biological Psychiatry*, *62*(5), 446–454. https://doi.org/10.1016/j.biopsych.2006.10.011

Mueller, E. M., Panitz, C., Hermann, C., & Pizzagalli, D. A. (2014). Prefrontal Oscillations during Recall of Conditioned and Extinguished Fear in Humans. *Journal of Neuroscience*, *34*(21), 7059–7066. https://doi.org/10.1523/JNEUROSCI.3427-13.2014

Noh, N. A., Fuggetta, G., Manganotti, P., & Fiaschi, A. (2012). Long Lasting Modulation of Cortical Oscillations after Continuous Theta Burst Transcranial Magnetic Stimulation. *PLOS ONE*, *7*(4), e35080. https://doi.org/10.1371/journal.pone.0035080

Okamoto, M., Dan, H., Sakamoto, K., Takeo, K., Shimizu, K., Kohno, S., Oda, I., Isobe, S., Suzuki, T., Kohyama, K., & Dan, I. (2004). Three-dimensional probabilistic anatomical cranio-cerebral correlation via the international 10–20 system oriented for transcranial functional brain mapping. *NeuroImage*, *21*(1), 99–111. https://doi.org/10.1016/j.neuroimage.2003.08.026

Pascual-Marqui, R. D. (2002). Standardized low-resolution brain electromagnetic tomography (sLORETA): Technical details. *Methods and Findings in Experimental and Clinical Pharmacology*, *24 Suppl D*, 5–12.

Putman, P., van Peer, J., Maimari, I., & van der Werff, S. (2010). EEG theta/beta ratio in relation to fear-modulated response-inhibition, attentional control, and affective traits. *Biological Psychology*, *83*(2), 73–78. https://doi.org/10.1016/j.biopsycho.2009.10.008

Quirk, G. J., & Beer, J. S. (2006). Prefrontal involvement in the regulation of emotion: Convergence of rat and human studies. *Current Opinion in Neurobiology*, *16*, 723–727. https://doi.org/10.1016/j.conb.2006.07.004

Rodenburg, S. C., Boor, M., Baas, J.M.P. (2022). *The role of the anterolateral prefrontal cortex in the regulation of defensive responses: a TMS study [Unpublished master's thesis].* Utrecht University

Sabatinelli, D., Keil, A., Frank, D. W., & Lang, P. J. (2013). Emotional perception: Correspondence of early and late event-related potentials with cortical and subcortical functional MRI. *Biological Psychology*, *92*(3), 513–519. https://doi.org/10.1016/j.biopsycho.2012.04.005

Schroeder, C. E., & Lakatos, P. (2009). Low-frequency neuronal oscillations as instruments of sensory selection. *Trends in Neurosciences*, *32*(1), 9–18. https://doi.org/10.1016/j.tins.2008.09.012

Schutter, D. J. L. G., & van Honk, J. (2006). A Standardized Motor Threshold Estimation Procedure for Transcranial Magnetic Stimulation Research. *The Journal of ECT*, *22*(3), 176–178. https://doi.org/10.1097/01.yct.0000235924.60364.27

Sperl, M. F. J., Panitz, C., Rosso, I. M., Dillon, D. G., Kumar, P., Hermann, A., Whitton, A. E., Hermann, C., Pizzagalli, D. A., & Mueller, E. M. (2019). Fear Extinction Recall Modulates Human Frontomedial Theta and Amygdala Activity. *Cerebral Cortex*, *29*(2), 701–715. https://doi.org/10.1093/cercor/bhx353

Sperl, M. F. J., Wroblewski, A., Mueller, M., Straube, B., & Mueller, E. M. (2021). Learning dynamics of electrophysiological brain signals during human fear conditioning. *NeuroImage*, *226*, 117569. https://doi.org/10.1016/j.neuroimage.2020.117569

Spielberger C. (1970). Manual for the State-trait Anxietry, Inventory. *Consulting Psychologist*. https://cir.nii.ac.jp/crid/1572261549249149184

Stewart, J. L., Bismark, A. W., Towers, D. N., Coan, J. A., & Allen, J. J. B. (2010). Resting frontal EEG asymmetry as an endophenotype for depression risk: Sex-specific patterns of frontal brain asymmetry. *Journal of Abnormal Psychology*, *119*, 502–512. https://doi.org/10.1037/a0019196

Tillman, R. M., Stockbridge, M. D., Nacewicz, B. M., Torrisi, S., Fox, A. S., Smith, J. F., & Shackman, A. J. (2018). Intrinsic functional connectivity of the central extended amygdala. *Human Brain Mapping*, *39*(3), 1291–1312. https://doi.org/10.1002/hbm.23917

van der Ploeg, Defares, & Spielberger, C. D. (1980). *Handleiding bij de Zelf-beoordelings Vragenlijst ZBV. Een nederlandstalige bewerking van de Spielberger State-Trait Anxiety Inventory*. Swets & Zeitlinger. https://library.wur.nl/WebQuery/wurpubs/73424

van Dijk, I., Klumpers, F., Kenemans, J. L., Hofman, D., Baas, J. M. P. (2017). *Critical Involvement of the Anterolateral Prefrontal Cortex in Startle Regulation [Unpublished manuscript]*. Utrecht University

Volman, I., Roelofs, K., Koch, S., Verhagen, L., & Toni, I. (2011). Anterior Prefrontal Cortex Inhibition Impairs Control over Social Emotional Actions. *Current Biology*, *21*(20), 1766–1770. https://doi.org/10.1016/j.cub.2011.08.050

Volman, I., Verhagen, L., Ouden, H. E. M. den, Fernández, G., Rijpkema, M., Franke, B., Toni, I., & Roelofs, K. (2013). Reduced Serotonin Transporter Availability Decreases Prefrontal Control of the Amygdala. *Journal of Neuroscience*, *33*(21), 8974–8979. https://doi.org/10.1523/JNEUROSCI.5518-12.2013

Wischnewski, M., & Schutter, D. J. L. G. (2015). Efficacy and Time Course of Theta Burst Stimulation in Healthy Humans. *Brain Stimulation*, *8*(4), 685–692. https://doi.org/10.1016/j.brs.2015.03.004

Appendix 1

Exploring the source of theta: 1.0.1.

To explore the potential differences in the theta source in cue onset and offset, we conducted a 5-way RMANOVA. In addition to the already mentioned factors: 'cTBS', 'Pre/Post', 'Threat/Safe', we also included factors: 'On/Off' (for cue onset and offset), and 'Electrode' (Fz and FCz). This analysis revealed that the Electrode did not interact with the On/Off ($F_{(1,27)} = 0.384$, $p = 0.540$), indicating that the source of theta was similar source for these electrodes during both cue onset and cue offset. Furthermore, Threat/Safe also did not interact with Electrode ($F_{(1,27)} = 0.170$, $p = 0.684$), indicating that both electrodes capture the difference between the cue conditions similarly. This interaction remained non-significant also when conducting a 4-way RMANOVA ('cTBS', 'Pre/Post', 'Threat/Safe', 'Electrode') on the cue onset (Threat/Safe * Electrode: $F_{(1,27)} = 0.138$, $p = 0.713$) and cue offset data separately (Threat/Safe * Electrode: $F_{(1,27)} = 0.066$, $p = 0.799$).

In addition to fronto-medial theta, we observed an increase in theta power also in electrodes that correspond with the alPFC area, and therefore, we conducted another 5-way RMANOVA to compare the fronto-medial electrodes (Fz for cue onset and FCz for cue offset) with the theta elicited by the pooled AF4 & Fp2 electrodes. The 2-level factor 'Electrode' represented: fronto-midline electrodes (Fz for the cue onset and FCz for the cue offset) and alPFC electrodes (pooled AF4 & Fp2). This analysis showed no interaction between Threat/Safe and Electrode ($F_{(1,27)} = 1.787$, $p = 0.192$). The interaction between the factors On/Off and Electrode reached significance ($F_{(1,27)} = 15.340$, $p < 0.001$), indicating that a different electrode has a higher power after cue onset and a different electrode after cue offset. After cue onset, the percentage change of pooled AF4 & Fp2 was higher than the percentage change of the fronto-midline theta (Fz electrode) (Figure 1). However, a 4-way RMANOVA on the cue onset data revealed no interaction between Electrode and Threat/Safe ($F_{(1,27)} = 0.183$, $p = 0.672$),

indicating that the electrode sites do not differ in their sensitivity to capture differences between the conditions. During the cue offset however, the percentage change of the fronto-midline theta (FCz electrode) was higher than the percentage change of the pooled AF4 & Fp2 (Figure 1). As Figure 1 indicates, the FCz electrode might capture the difference between threat and safe condition slightly better than the pooled AF4 & Fp2. However, the 4-way RMANOVA on the cue offset data did not reveal a significant interaction between the Electrode and Threat/Safe ($F_{(1,27)} = 2.826$, $p = 0.104$).

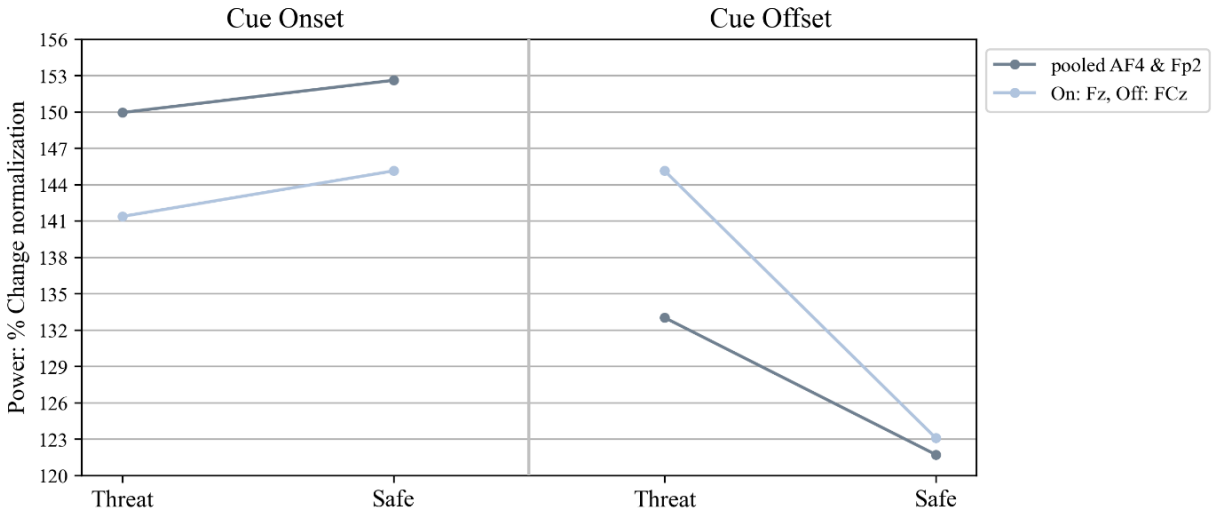

Figure 1. *Exploring the effects of the electrodes on theta oscillations after cue onset and cue offset*

Exploring the source of theta: 1.0.2.

In order to explore the potential differences in the source of theta at cue onset and offset more precisely, we conducted a further 6-way RMANOVA that included a wide array of 15 electrodes (Fp1, Fpz, Fp2, AF3, AFz, AF4, F1, Fz, F2, FC1, FCz, FC2, C1, Cz, C2). These factors were included in the analysis: 'cTBS', 'Pre/Post', 'Threat/Safe', 'On/Off', 'Electrode position: Fp/AF/F/FC/C', 'Electrode laterality: Left/Middle/Right'. This analysis did not reveal an interaction between the factors Threat/Safe and Electrode position ($F_{(1,27)} = 1.777$, $p = 0.166$), which indicates that the sensibility of electrode positions to capture the difference between

conditions does not significantly differ. However, the interaction between the factors On/Off and Electrode position reached statistical significance ($F_{(1,27)} = 16.381$, $p < 0.001$). This indicates that the source of theta for cue onset and cue offset might differ. Moreover, a significant interaction was also observed for the factors Threat/Safe and Electrode laterality ($F_{(1,27)} = 5.706$, $p = 0.009$), which indicates that the laterality of the selected electrodes influences the sensitivity of the electrode to capture the difference between the threat and safe condition. On the other hand, the interaction between the On/Off and Electrode laterality did not reach statistical significance ($F_{(1,27)} = 0.165$, $p = 0.849$), indicating that the laterality of the electrode does not distinguish between the potential difference in the source of theta in cue onset and cue offset.

A follow-up 5-way RMANOVA was conducted on the cue onset (Figure 2) and cue offset (Figure 3) data separately, with the other factors identical to the ones described in the previous analysis. The cue onset data revealed that the interaction between Threat/Safe and Electrode position was nonsignificant ($F_{(1,27)} = 0.735$, $p = 0.577$), indicating that the sensitivity to detect differences between the conditions did not differ among the electrode position. Furthermore, the three way interaction between the factors Threat/Safe, Electrode position and Electrode laterality was also nonsignificant ($F_{(1,27)} = 0.750$, $p = 0.648$), which implies that differences in the sensitivity of electrodes to distinguish between conditions does not differ. For the cue offset data, the interaction between Threat/Safe and Electrode position did not reach statistical significance ($F_{(1,27)} = 2.021$, $p = 0.123$), which indicates that the sensitivity of the electrode position to distinguish between the conditions does not differ. However, we observed a statistically significant interaction between the 3 factors: Threat/Safe, Electrode position, and Electrode laterality ($F_{(1,27)} = 2.768$, $p = 0.031$). This implies that some electrodes distinguish between the conditions better than other electrodes.

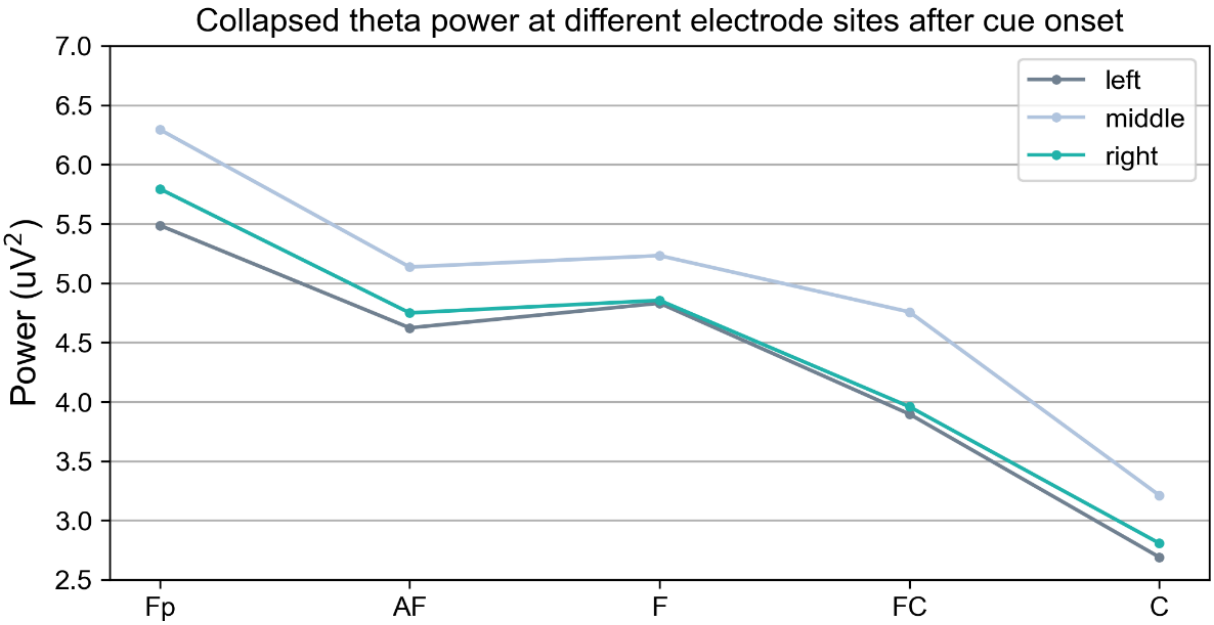

Figure 2. *Collapsed exported theta power (4 to 8 Hz) across all participants and conditions for cue onset. Selected time window: 50 to 450ms.*

After collapsing the exported theta power across conditions and participants for the cue onset, the highest theta power was recorded at the Fpz electrode (Figure 2). However, to be consistent with other studies that report the involvement of fronto-midline theta increase in fear expression (Mueller et al., 2014; Sperl et al., 2019), the electrode Fz was originally selected for statistical analysis. We also explored the Fpz electrode. The highest power increase occurred in the same time window as for Fz electrode: 50 to 450ms. A 3-way RMANOVA with the factors 'cTBS', 'Pre/Post', 'Threat/Safe' on the percentage change normalized data exported from Fpz electrode also showed a non-significant main effect of the factor Threat/Safe ($F_{(1,27)} = 0.563$, $p = 0.459$). As an exploratory analysis, we also applied a separate 3-way RMANOVAs with the same factors as for the Fpz/Fz analysis on each of the fifteen electrodes included in the above-mentioned array. Because of the multiple tests, Bonferroni correction is necessary to prevent the multiple comparisons problem (Field, 2018). These analyses revealed that the Threat/Safe conditions did not statistically differ in any of these electrodes ($p > 0.1$).

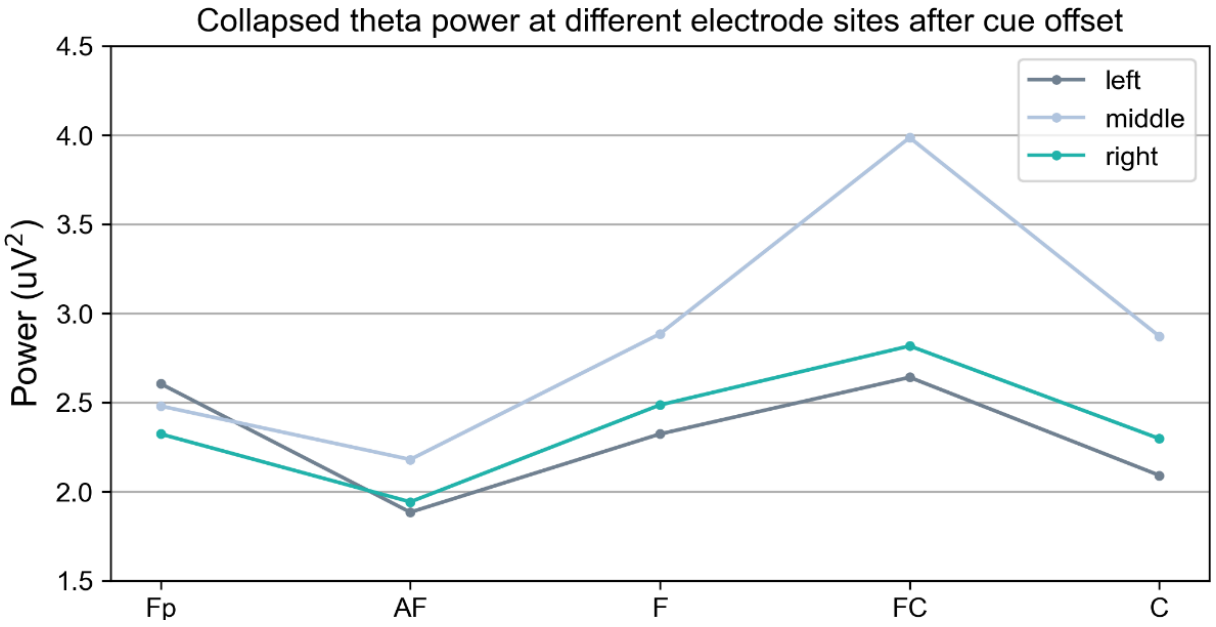

Figure 3. *Collapsed exported theta power (4 to 8 Hz) across all participants and conditions for cue offset. Selected time window: 50 to 450ms.*

The FCz electrode was selected for statistical analysis, which is also the electrode with the highest power increase (Figure 3).